Supporting Information

Stimuli responsive gelation of tert-butylacetic acid based LMOGs – applications in remediation of marine oil spill, dye removal and heavy metal sensing

Varsha Bhardwaj, Ajaykumar M, Patel, Amar Ballabh*

Department of Chemistry, Faculty of Science, The Maharaja Sayajirao University of Baroda, Vadodara-390002, Gujarat (INDIA).

Contents –

Solvents utilized in gelation trials

Sr.	Solvent type	Nature	Solvents
1.	Polar	Protic	Water Methanol Ethanol Isopropanol n-butanol tert-butanol **propan-1,2-diol** hexan-1-ol octan-2-ol decan-1-ol polyethylene glycol
2.	Polar	Aprotic	Acetone Ethyl acetate **Dimethyl Sulfoxide** Dimethyl Formamide Acetonitrile Tetrahydrofuran Diethyl ether Dibenzyl ether Diisopropyl ether
2.	Halogenated	Aprotic	Chloroform Dichloromethane Carbon tetrachloride
3.	Hydrocarbon	Aliphatic	Petroleum ether n-Hexane n-Heptane **n-Octane** **n-Decane** **n-Dodecane** **n-Hexadecane** Cyclohexane Decalin Petrol **Diesel** **Kerosene** **Engine oil** **Cooking oil** **Silicone oil**
4.	Aromatic		Benzene Toluene Chlorobenzene

			Bromobenzene Nitrobenzene Xylenes (o-,m-,p-)
5.	Mixtures	Aliphatic+Aromatic	n-hexane + benzene (1:1) n-heptane + benzene (1:1) n-octane + benzene (1:1) decane + benzene (1:1) dodecane + benzene (1:1) hexadecane + benzene (1:1) n-hexane + toluene (1:1) n-heptane + toluene (1:1) n-octane + toluene (1:1) decane + toluene (1:1) dodecane + toluene (1:1) hexadecane + toluene (1:1) n-hexane + chlorobenzene (1:1) n-heptane + chlorobenzene (1:1) n-octane + chlorobenzene (1:1) decane + chlorobenzene (1:1) dodecane + chlorobenzene (1:1) hexadecane + chlorobenzene (1:1) n-hexane + bromobenzene (1:1) n-heptane + bromobenzene (1:1) n-octane + bromobenzene (1:1) decane + bromobenzene (1:1) dodecane + bromobenzene (1:1) hexadecane + bromobenzene (1:1) n-hexane + nitrobenzene (1:1) n-heptane + nitrobenzene (1:1) n-octane + nitrobenzene (1:1) decane + nitrobenzene (1:1) dodecane + nitrobenzene (1:1) hexadecane + nitrobenzene (1:1)

Table S1 List of solvents employed for gelation trials
Solvents in bold gave gelation

T_{gel} vs. concentration plots

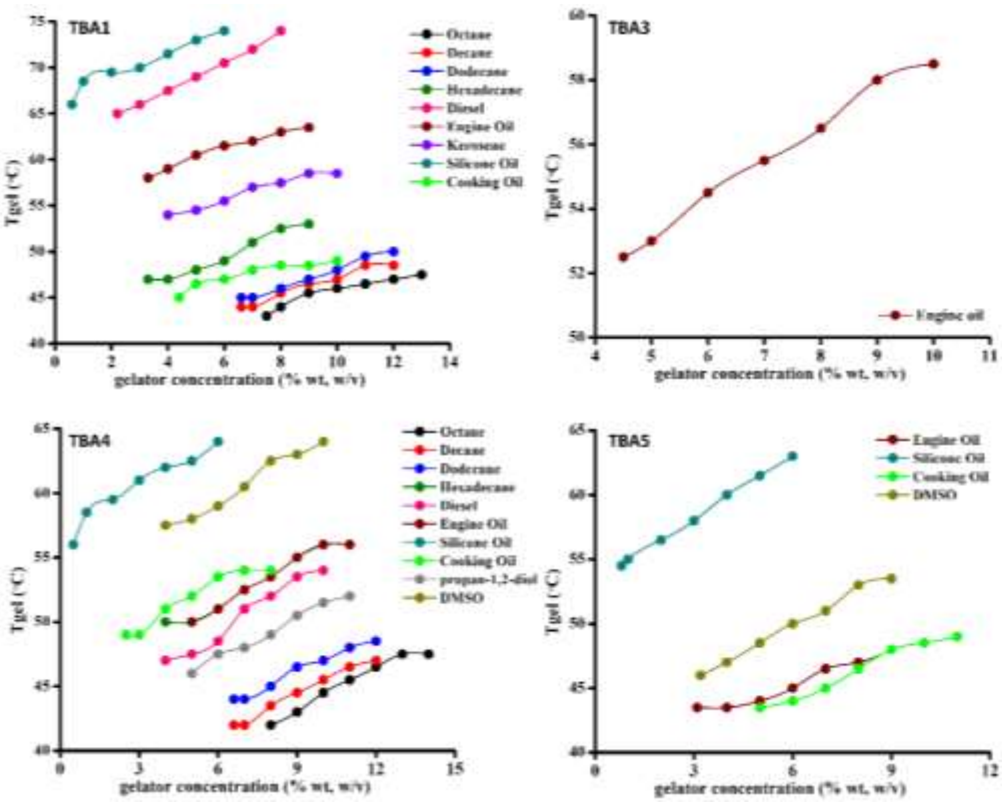

Figure S1 Tgel vs. concentration plots for all gels

Calculation of ΔH for aliphatic solvents

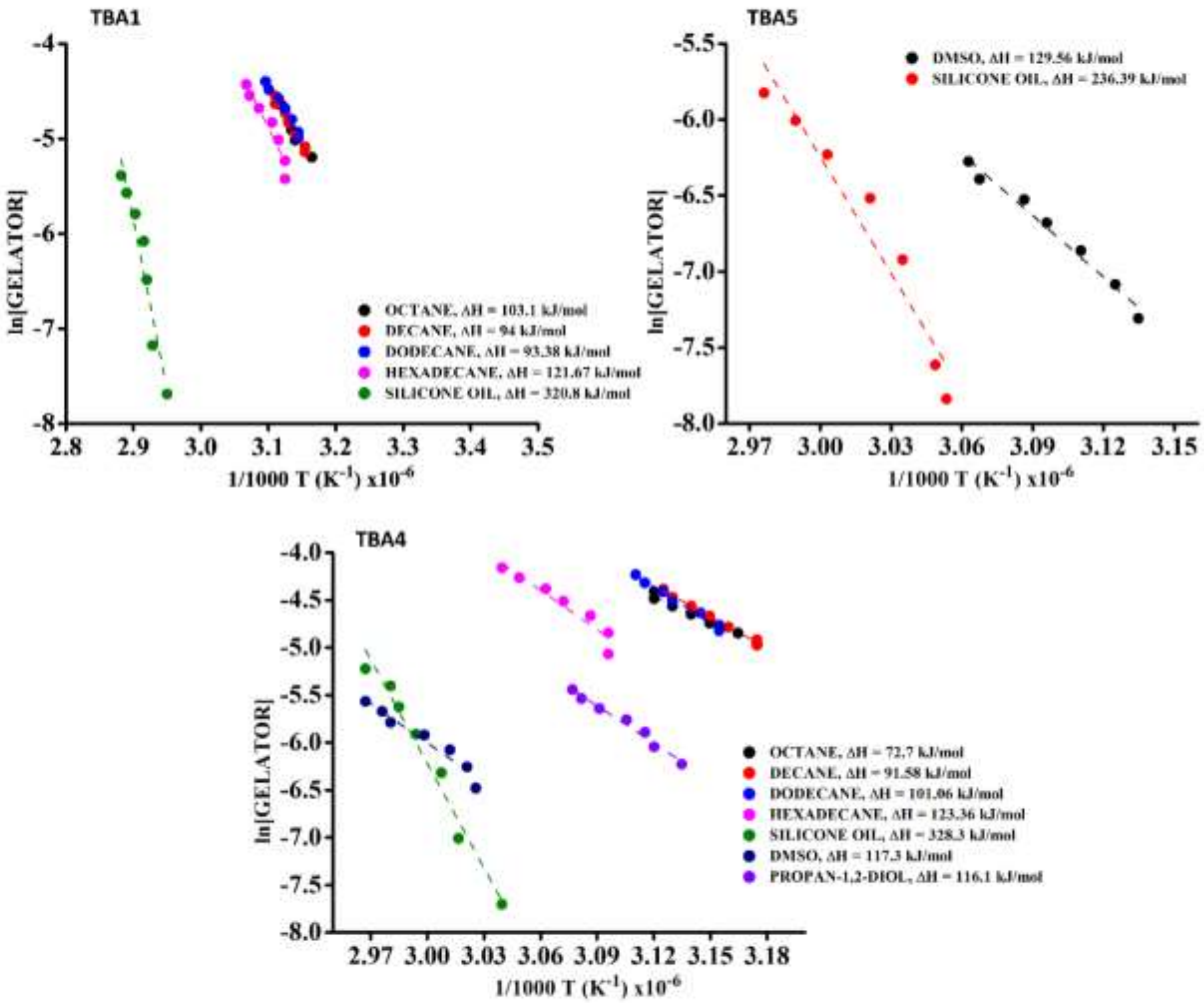

Figure S2 ΔH values for all gels

Toxic Dye Removal plots

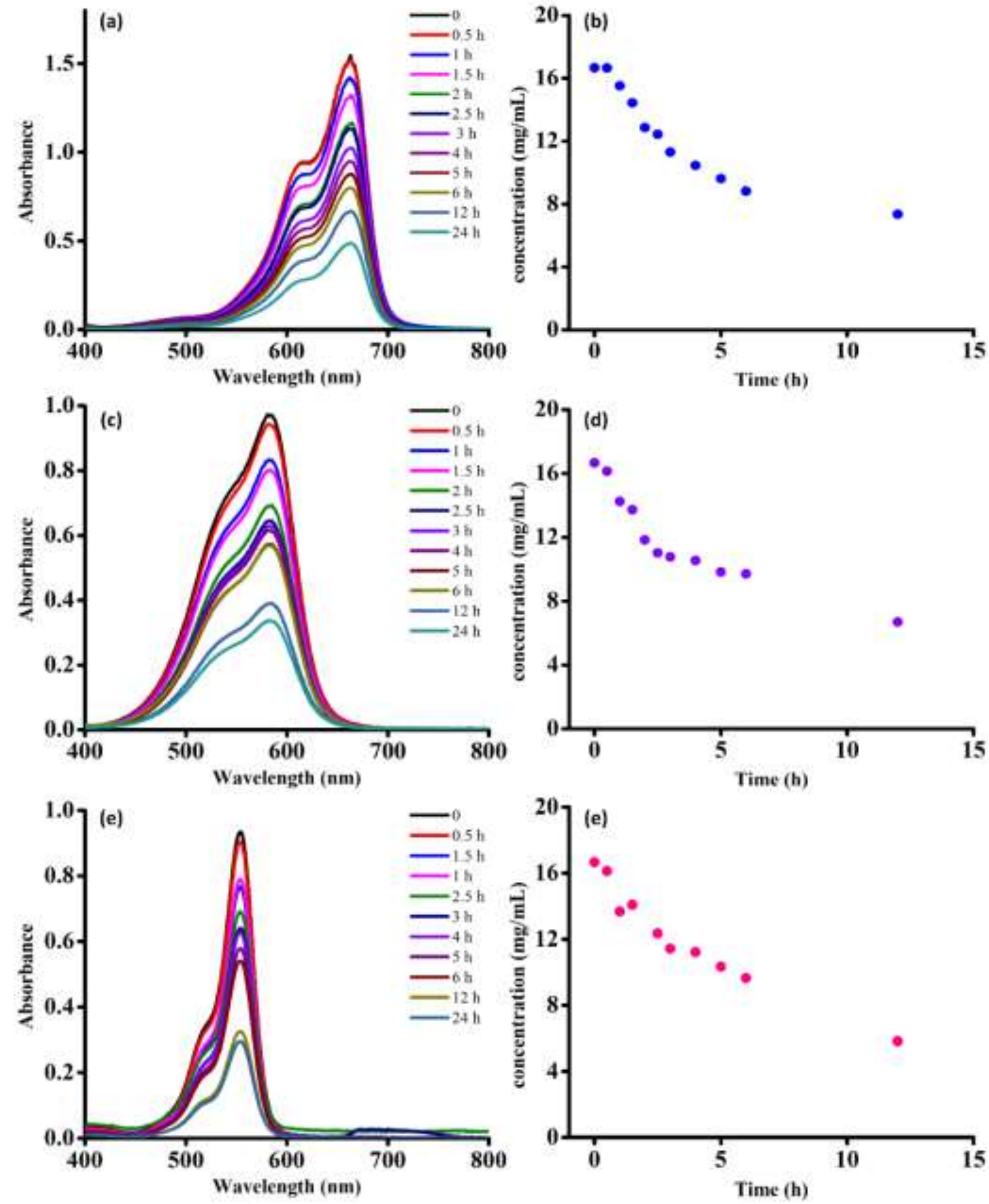

Figure S3 Time dependent absorption studies for **TBA4** in aqueous solution of 1.5 mL which contains (a) methylene blue dye at an initial concentration of 25mg/1.5 mL and (b) concentration-time correlation at 664 nm, (c) crystal violet dye at an initial concentration of 25mg/1.5 mL and (d) concentration-time correlation at 583 nm, (e) Rhodamine B dye at an initial concentration of 20mg/1.5mL, in presence of 1 mL of diesel congealed on the water surface using 5% w/v of **TBA4** and (f) its concentration-time correlation at 554 nm.

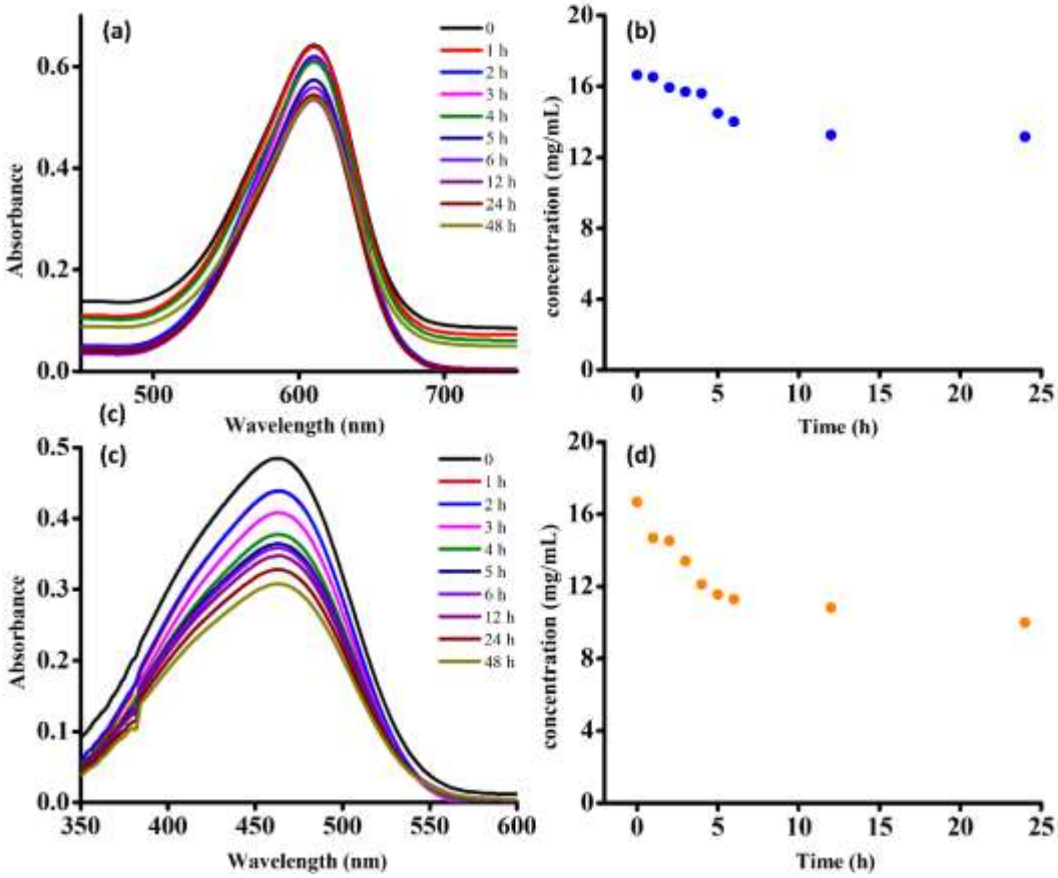

Figure S4 Time dependent absorption studies for **TBA1** in aqueous solution of 1.5 mL which contains (a) indigo carmine dye at an initial concentration of 25mg/1.5 mL and (b) concentration-time correlation at 610 nm, (c) methyl orange dye at an initial concentration of 25mg/1.5 mL, in presence of 1 mL of diesel congealed on the water surface using 5% w/v of **TBA1** and (d) its concentration-time correlation at 462 nm

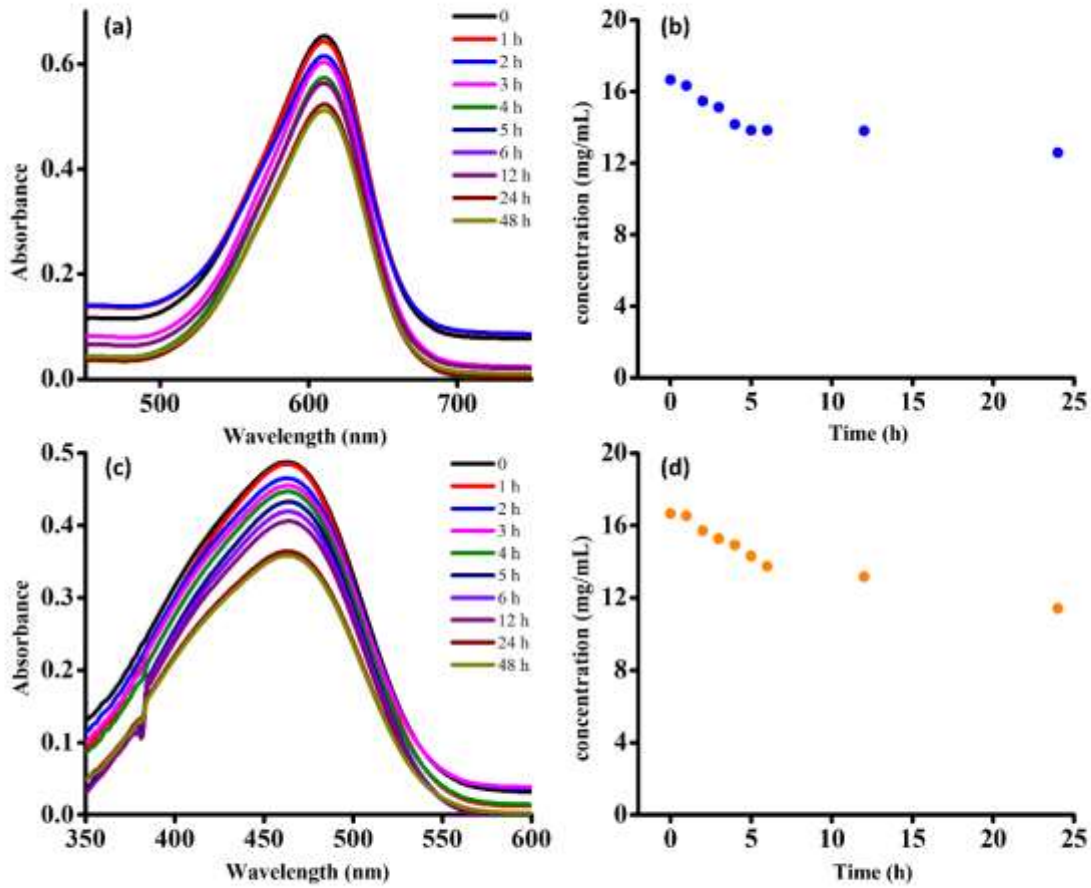

Figure S5 Time dependent absorption studies for **TBA4** in aqueous solution of 1.5 mL which contains (a) indigo carmine dye at an initial concentration of 25mg/1.5 mL and (b) concentration-time correlation at 610 nm, (c) methyl orange dye at an initial concentration of 25mg/1.5 mL, in presence of 1 mL of diesel congealed on the water surface using 5% w/v of **TBA4** and (d) its concentration-time correlation at 462 nm

Metal sensing studies

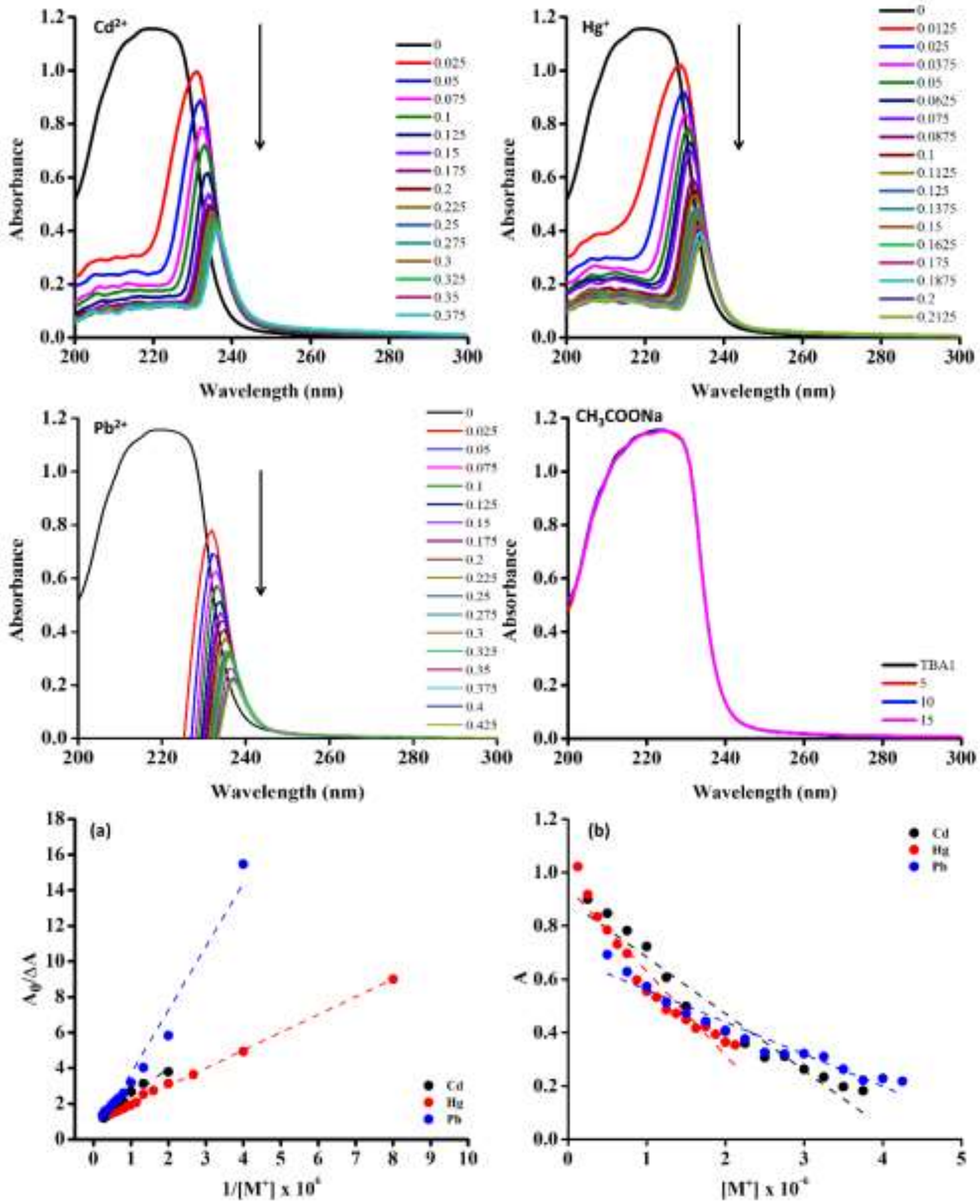

Figure S6 Change in absorbance of **TBA1** with increasing concentrations of cadmium(II), mercury(II) and lead (II), control experiment with sodium acetate; (a) Benesi–Hildebrand plot and (b) detection limit of all metal ions with **TBA1**

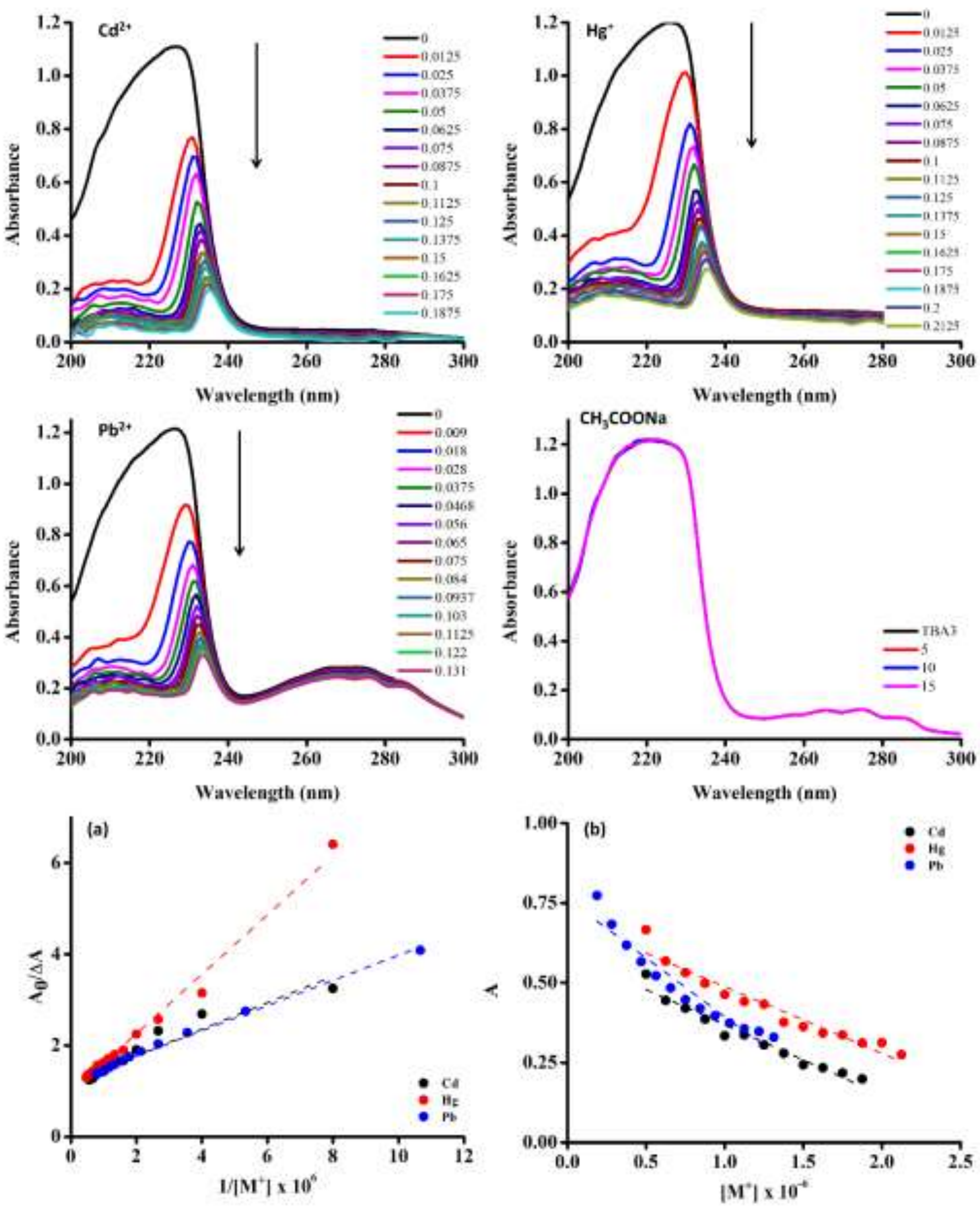

Figure S7 Change in absorbance of **TBA3** with increasing concentrations of cadmium(II), mercury(II) and lead (II), control experiment with sodium acetate; (a) Benesi–Hildebrand plot and (b) detection limit of all metal ions with **TBA3**

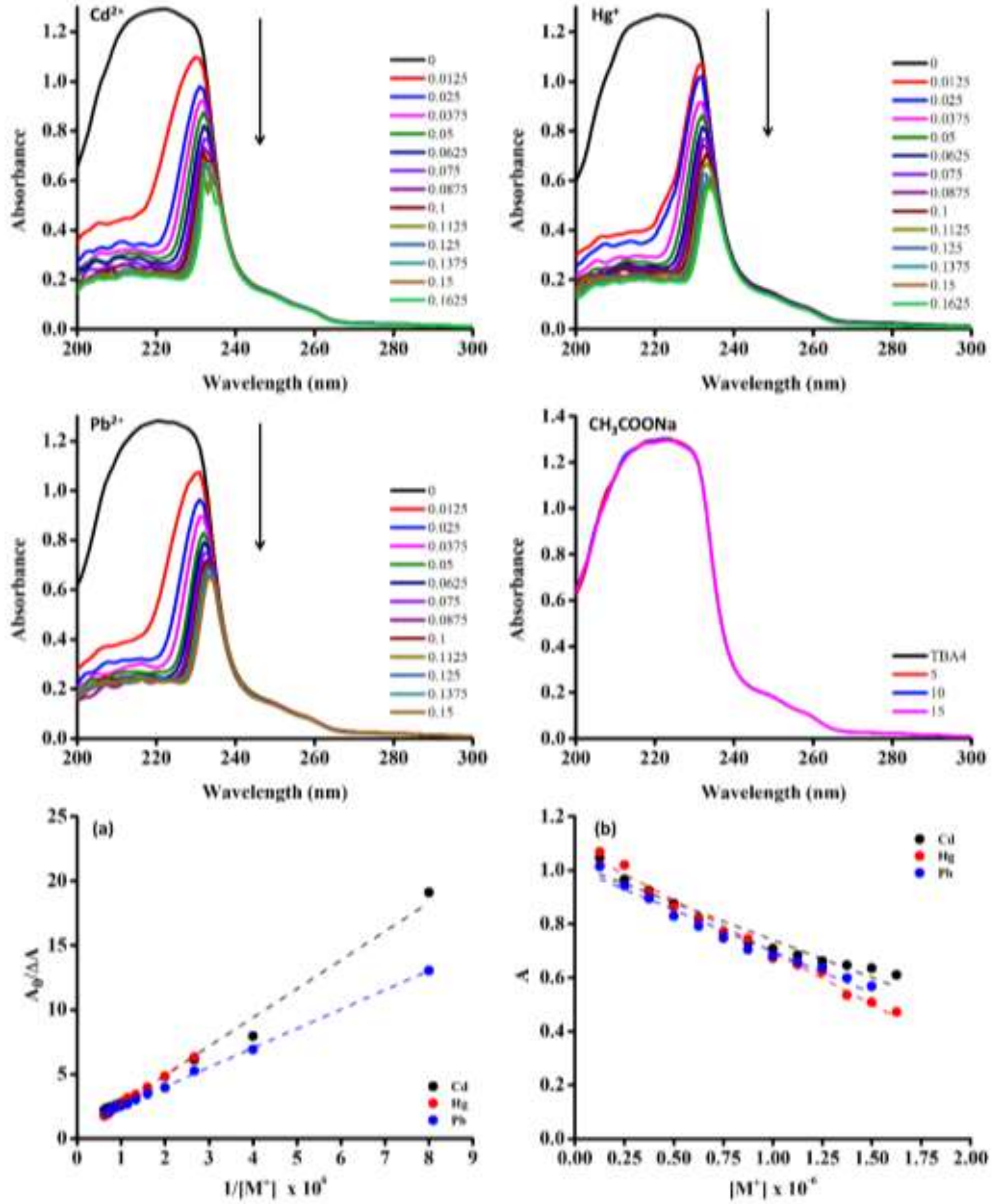

Figure S8 Change in absorbance of **TBA4** with increasing concentrations of cadmium(II), mercury(II) and lead (II), control experiment with sodium acetate; (a) Benesi–Hildebrand plot and (b) detection limit of all metal ions with **TBA4**

Job's plots

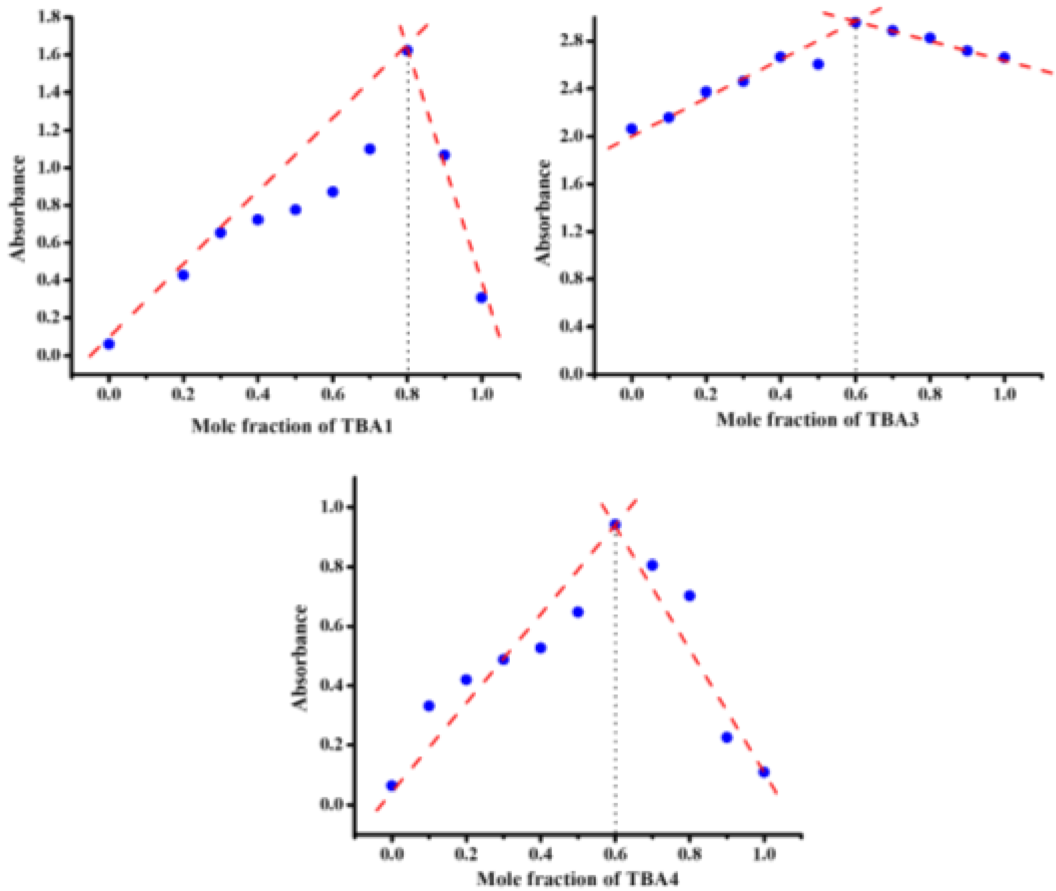

Figure S9 Job's plots for compounds **TBA1**, **TBA3** and **TBA4** in presence of mercuric ions

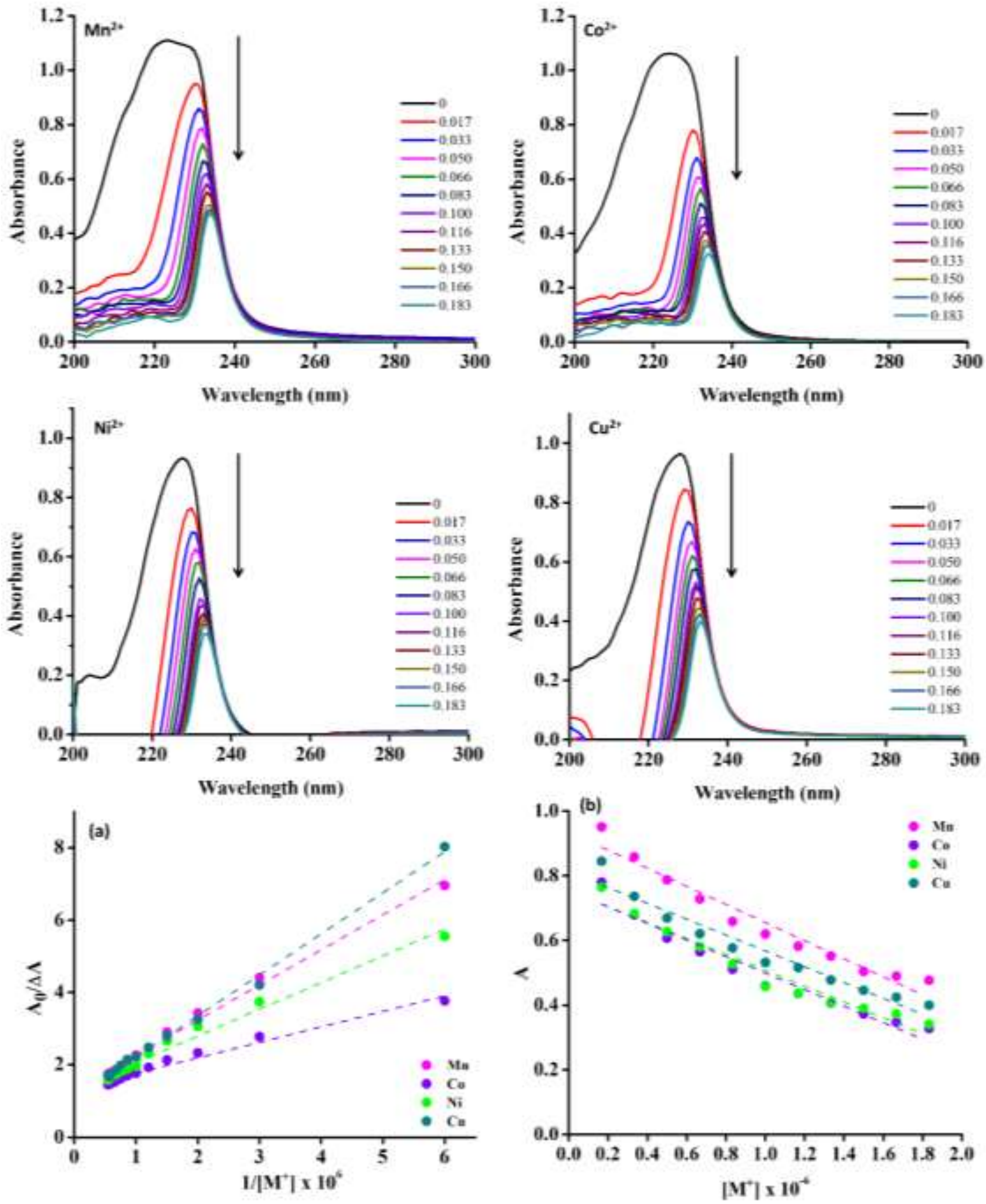

Figure S10 Change in absorbance of **TBA1** with increasing concentrations of manganese(II), cobalt(II), nickel(II) and copper(II) ions, (a) Benesi–Hildebrand plot and (b) detection limit of all metal ions with **TBA1**

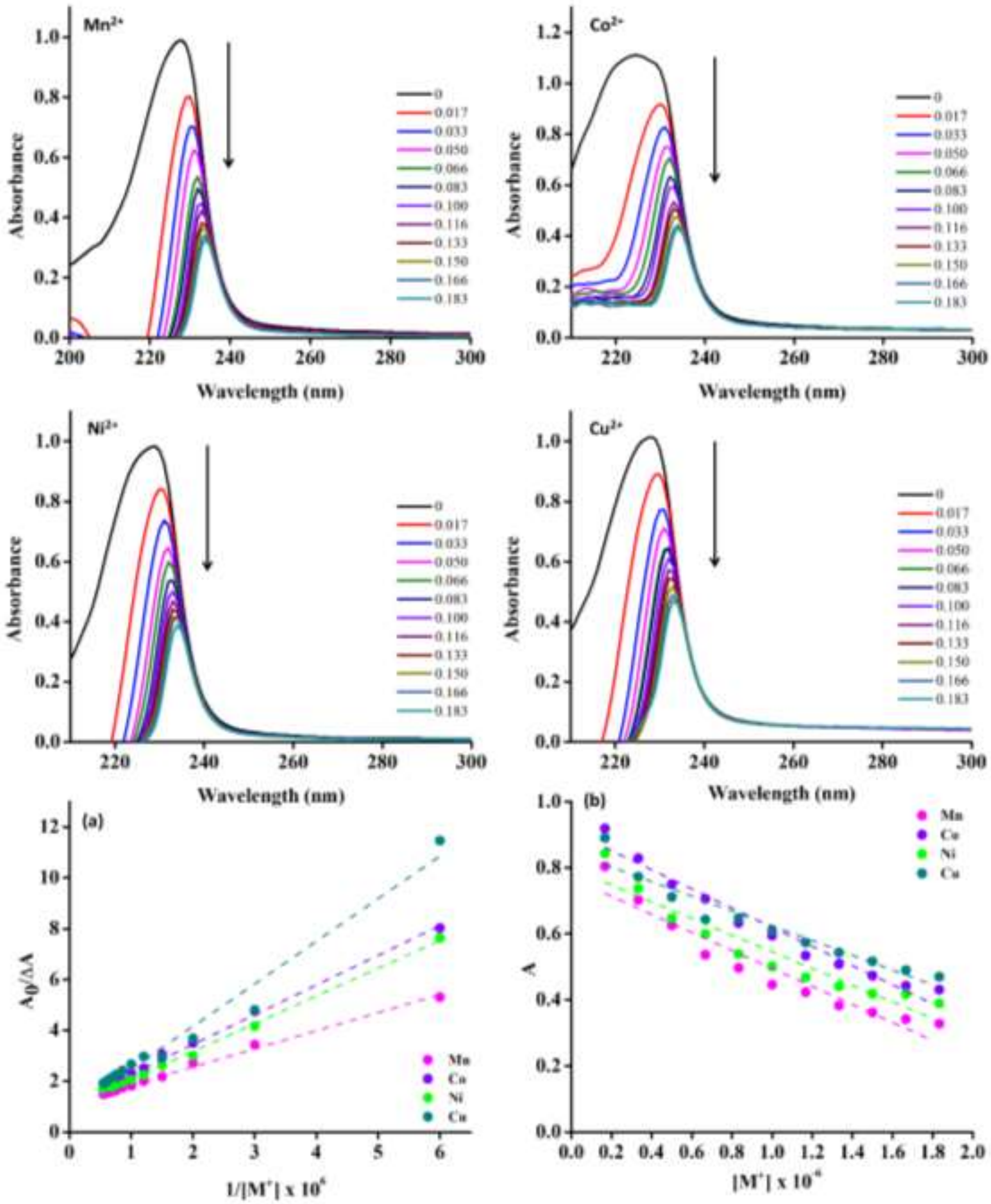

Figure S11 Change in absorbance of **TBA3** with increasing concentrations of manganese(II), cobalt(II), nickel(II) and copper(II) ions, (a) Benesi–Hildebrand plot and (b) detection limit of all metal ions with **TBA3**

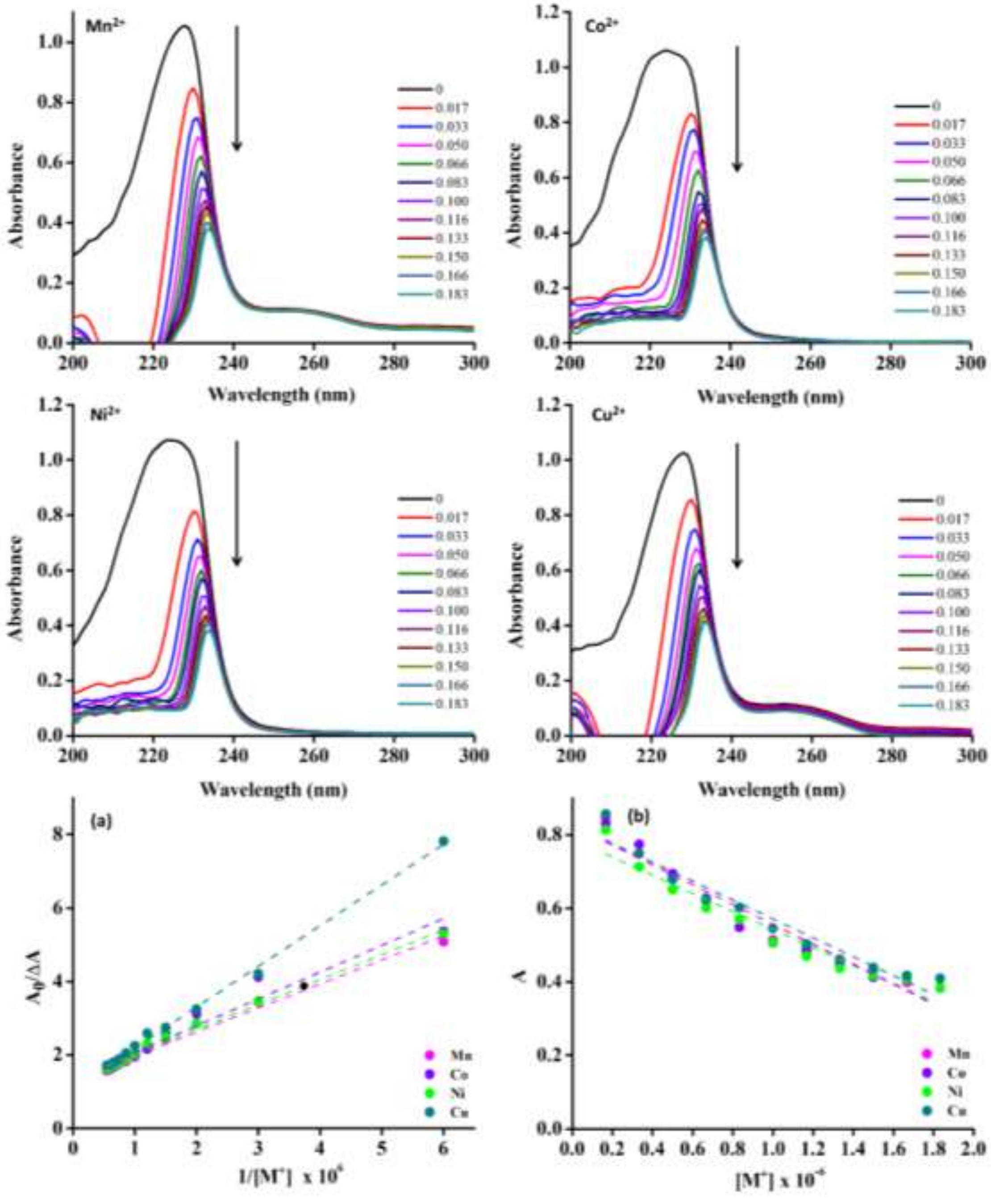

Figure S12 Change in absorbance of **TBA4** with increasing concentrations of manganese(II), cobalt(II), nickel(II) and copper(II) ions, (a) Bnesi–Hildebrand plot and (b) detection limit of all metal ions with **TBA4**

LOD and Ka values for all the heavy metals tested

Table S2

	TBA1		TBA3		TBA4	
	Detection Limit $\times 10^{-6}$ M	K_a $\times 10^{6}$ M^{-1}	Detection Limit $\times 10^{-6}$ M	K_a $\times 10^{6}$ M^{-1}	Detection Limit $\times 10^{-6}$ M	K_a $\times 10^{6}$ M^{-1}
Mn	0.433	1.345	0.566	1.600	0.462	2.025
Co	0.441	3.141	0.388	0.944	0.485	1.841
Ni	0.431	1.792	0.619	0.911	0.471	2.002
Cu	0.468	0.955	0.541	0.484	0.461	0.984

1H NMR in presence of metal salts

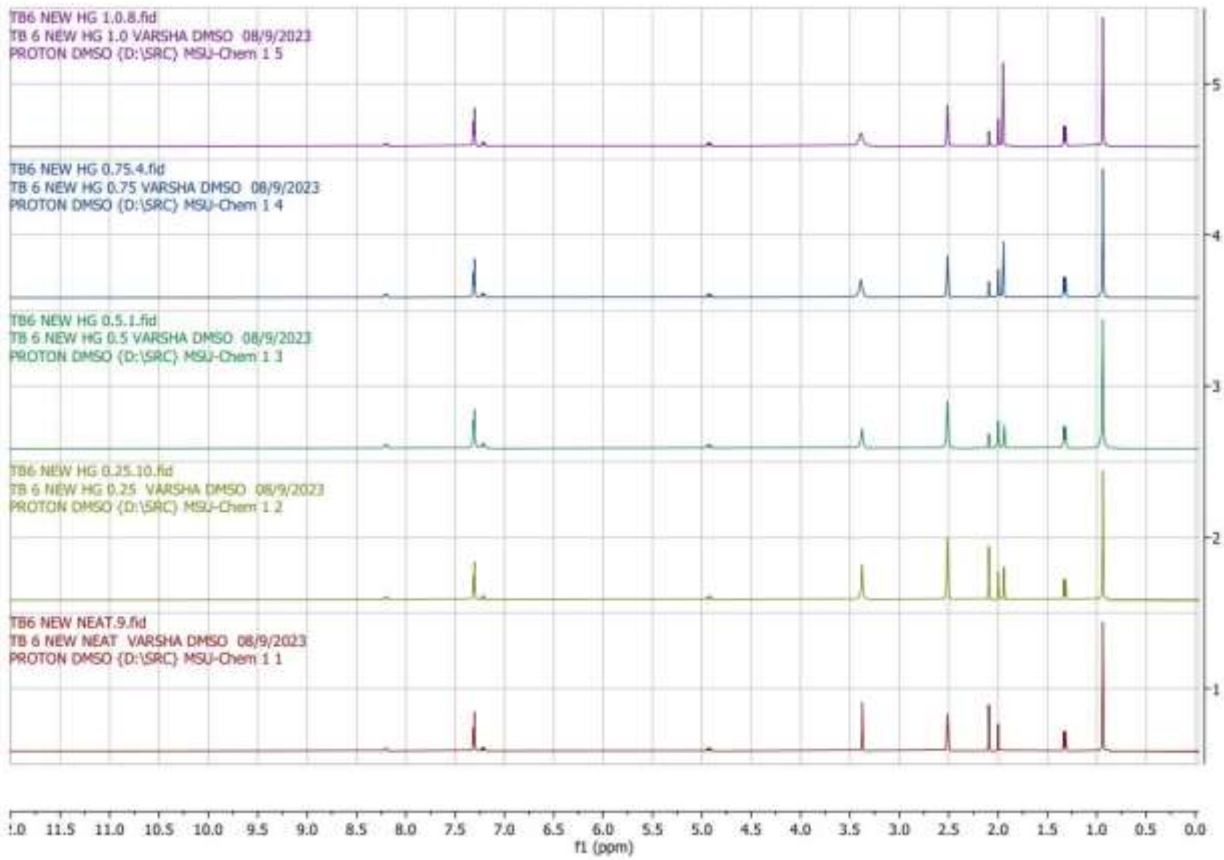

Figure S13 Proton NMR of TBA1 in presence of 0.25, 0.5, 0.75 and 1.0 mole equivalents of mercuric acetate salt in DMSO-d6

FT-IR in presence of mercuric metal salts

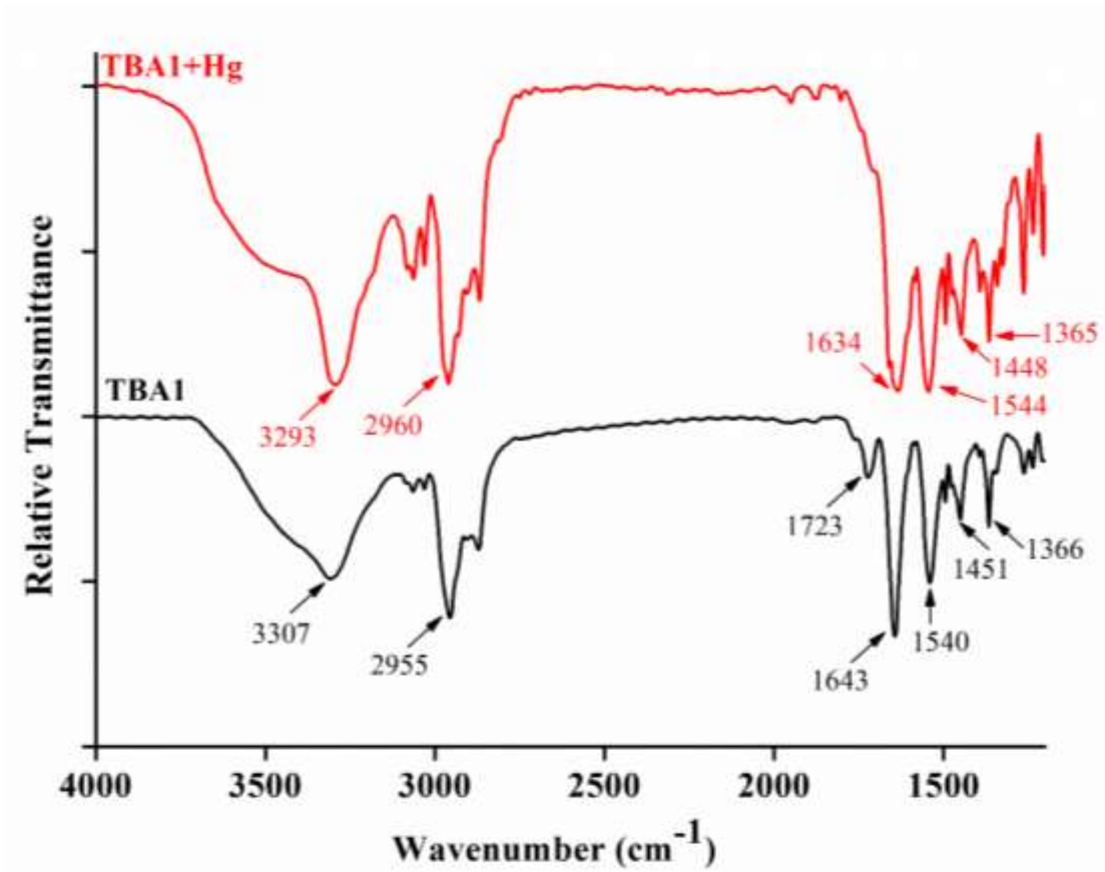

Figure S14 FT-IR of **TBA1** in presence of mercuric acetate salt in THF

Rheology

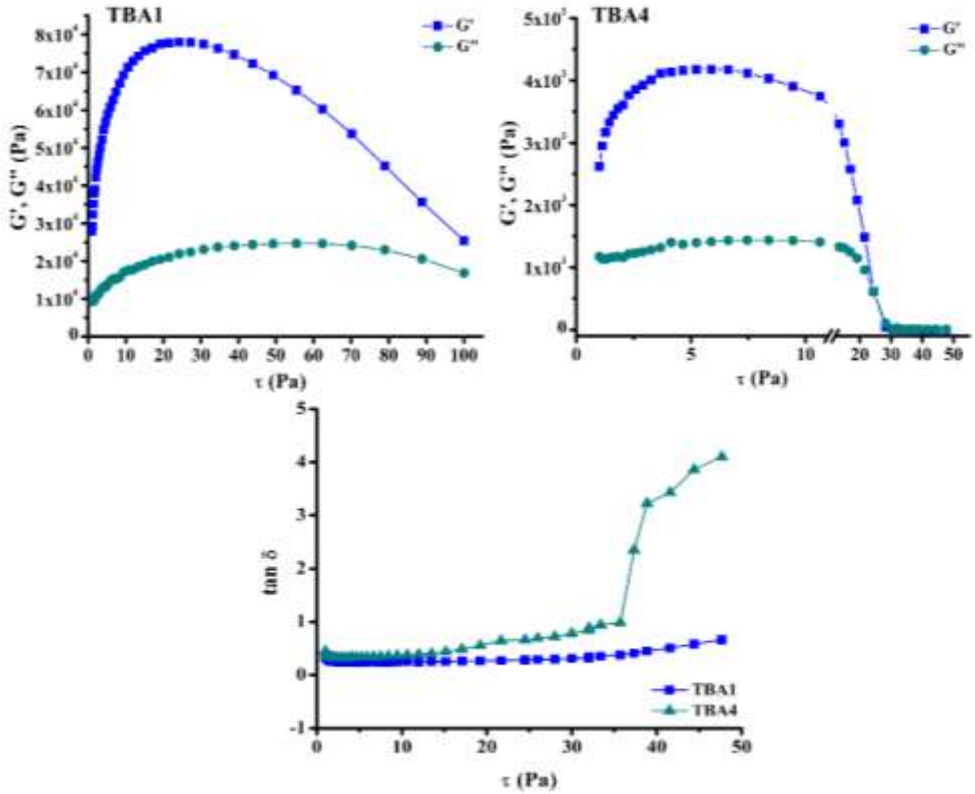

Figure S15 Rheological behavior of the gels in diesel and trends in tan δ values

Comparative IR spectra of Compound TB1 with xerogel, gel solution phase (solvent used – n-octane)

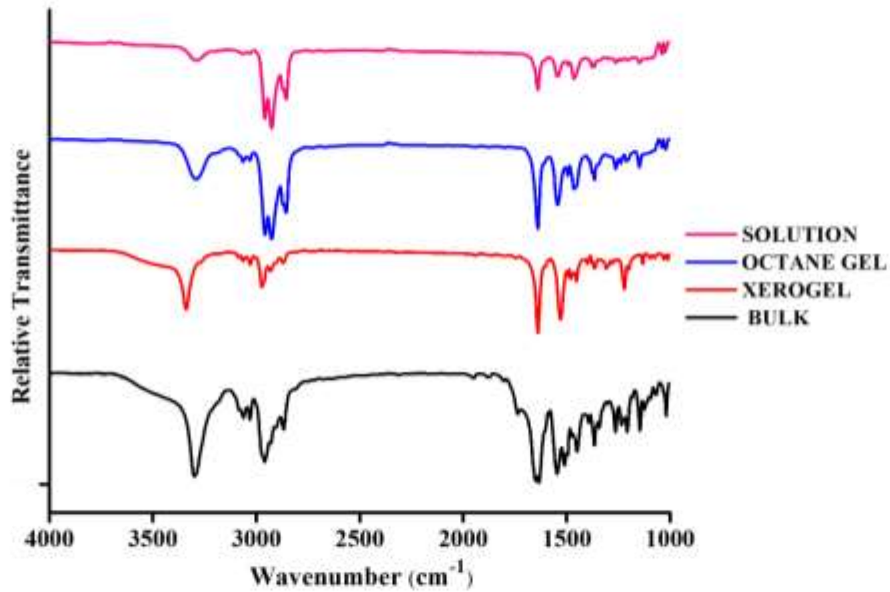

Figure S16 Comparison of FT-IR spectra between different forms of **TBA1**

Comparative PXRD patterns

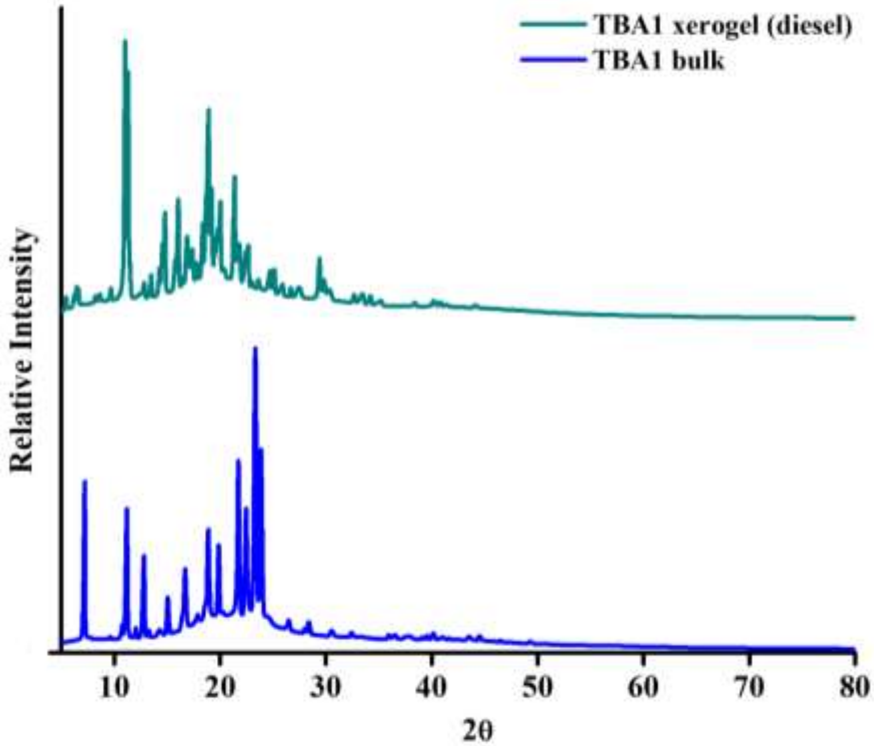

Figure S17 Comparative PXRD spectra of **TBA1**

Crystallographic Parameters

Table S3

Code	TBA4
Empirical formula	$C_{48}H_{92}N_4O_4$
Formula weight	789.25
Temperature/K	140.00
Crystal system	monoclinic
Space group	$P2_1/c$
a/Å	23.20(3)
b/Å	10.861(13)
c/Å	10.066(13)
α/°	90
β/°	90.07(4)
γ/°	90
Volume/Å^3	2537(6)
Z	2
ρ_{calc}g/cm^3	1.033
μ/mm^{-1}	0.064
F(000)	880.0
Crystal size/mm^3	0.7 x 0.5 x 0.3
Radiation	MoKα (λ = 0.71073)
2Θ range for data collection/°	4.14 to 50.49
Index ranges	-27 ≤ h ≤ 27, -12 ≤ k ≤ 12, -11 ≤ l ≤ 9
Reflections collected	14743
Independent reflections	4443 [Rint = 0.2156, Rsigma = 0.2625]
Data/restraints/parameters	4443/0/260
Goodness-of-fit on F^2	0.867
Final R indexes [I>=2σ (I)]	R1 = 0.0771, wR2 = 0.1694
Final R indexes [all data]	R1 = 0.2538, wR2 = 0.2612
Largest diff. peak/hole / e Å^{-3}	0.17/-0.17
CCDC No.	2221607

Analytical Data

Compound TBA1 (N-(1-phenylethyl)- 3,3-dimethylbutanamide). M.P.= 60℃, ^{1}H NMR (400 MHz, $CDCl_3$, TMS) = δ (ppm) 7.766-7.322 (*m*, 5H, 5(CH) ar), δ 5.660 (*s*, 1H, -CONH), δ 5.199-5.051 (*m*, 1H, (CH)), δ 2.063 (*s*, 2H, CH_2), δ 1.579-1.562 (*d*, 1H, CH), δ 1.517-1.499(*d*, 3H, CH_3), 1.040 (*s*, 9H, 3(CH_3)). ^{13}C = δ (ppm) 171, 159, 143, 142, 128, 127, 126, 50, 49, 48, 31, 29, 21.

FT-IR, cm^{-1} (KBr) – 3299, 3062. 3031, 2960, 2808, 1736, 1634, 1545, 1510, 1449, 1393, 1385, 1342, 1263, 1234, 1207, 1145, 1018, 907, 763, 697, 623, 541.

Compound TBA2 (N-(3-ethynylphenyl)-3,3-dimethylbutanamide). M.P.= 98℃, ^{1}H NMR (400 MHz, $CDCl_3$, TMS) = δ (ppm) 7.654 (*s*, 1H, (CH) ar), δ 7.572-7.553 (*d*, 1H, (CH) ar), δ 7.299-7.215 (*m*, 2H, 2(CH) ar), δ 3.077 (*s*, 1H, ≡CH), δ 2.237 (*s*, 2H, CH_2), δ 1.114 (*s*, 9H, 3(CH_3)). ^{13}C = δ (ppm) 170, 137, 129, 127, 123, 122, 120, 83, 51, 31, 29.

FT-IR, cm^{-1} (KBr) – 3431, 3292, 3067, 2961, 2361, 1651, 1580, 1554, 1474, 1419, 1366, 1337, 1277, 1152, 1132, 1041, 976, 954, 885, 793, 763, 690, 665, 633.

Compound TBA3 (N-(1-benzylpiperidin-4-yl)-3,3-dimethylbutanamide). M.P.= 96℃, ^{1}H NMR (400 MHz, $CDCl_3$, TMS) = δ (ppm) 7.330-7.264 (*m*, 5H, 5(CH) ar), δ 5.311-5.292 (*d*, 1H, -CONH), δ 3.861-3.786 (*m*, 1H, (CH)), δ 3.500 (*s*, 2H, CH_2)), δ 2.839-2.811 (*d*, 2H, 2($C\underline{H}_2$)), δ 2.149-2.095 (*m*, 2H, 2($C\underline{H}_2$)), δ 2.026 (*s*, 2H, CH_2), δ 1.932-1.905 (*m*, 2H, 2($C\underline{H}_2$)), δ 1.502-1.405 (*m*, 2H, 2($C\underline{H}_2$)), δ 1.031 (*s*, 9H, 3(CH_3)). ^{13}C = δ (ppm) 171, 138, 129, 128, 127, 63, 52, 50, 48, 46, 35, 32, 30, 29.

FT-IR, cm^{-1} (KBr) – 3290, 3082, 3029, 2955, 2866, 2802, 1634, 1554, 1493, 1448, 1393, 1364, 1273, 1245,1201, 1154, 1141, 1092, 1028, 863, 791, 743, 731, 698, 643.

Compound TBA4 (N-cyclohexyl-3,3-dimethylbutanamide). M.P.= 88℃, ^{1}H NMR (400 MHz, $CDCl_3$, TMS) = δ (ppm) 5.478 (*s*, 1H, -CONH), δ 3.756-3.713 (*m*, 1H, (CH)), δ 1.987 (*s*, 2H, CH_2), δ 1.898-1.859 (*m*, 2H, 2($C\underline{H}_2$)), δ 1.734-1.380 (*m*, 2H, 2($C\underline{H}_2$)), δ 1.372-1.342 (*m*, 1H, $C\underline{H}_2$), δ 1.333-1.101 (*m*, 2H, 2($C\underline{H}_2$)), δ 1.081-1.036 (*m*, 3H, 3($C\underline{H}_2$)), δ 0.997 (*s*, 9H, 3(CH_3)). ^{13}C = δ (ppm) 170, 159, 50, 48, 47, 33, 32, 30, 29, 25, 24.

FT-IR, cm^{-1} (KBr) – 3307, 3077, 2952, 2933, 2853, 1637, 1547, 1447, 1365, 1346, 1300, 1273, 1256, 1239, 1202, 1153, 1100, 993, 891, 719, 622, 554.

Compound TBA5 (N-hexadecyl-3,3-dimethylbutanamide). M.P.= 54℃, ^1H NMR (400 MHz, $CDCl_3$, TMS) = δ (ppm) 5.431 (*s*, 1H, -CONH), δ 3.261-3.211 (*m*, 2H, CH_2), δ 2.042 (*s*, 2H, CH_2), δ 1.55-1.45 (*m*, 2H, CH_2), δ 1.288-1.258 (*m*, 28H, 14(CH_2)), δ 1.039 (*s*, 9H, 3(CH_3)), δ 0.886 (*t*, 3H, $C\underline{H}_3$). ^{13}C = δ (ppm) 171, 50, 39, 31, 30, 29.8-29.3, 26.9, 22, 14.

FT-IR, cm^{-1} (KBr) – 3301, 3062, 2915, 2849, 1633, 1543, 1474, 1393, 1365, 1333, 1265, 1232, 1201, 1145, 1039, 958, 716, 659, 620.

Compound TBA6 (N-dodecyl-3,3-dimethylbutanamide). M.P.= 43℃, ^1H NMR (400 MHz, $CDCl_3$, TMS) = δ (ppm) 5.409 (*s*, 1H, -CONH), δ 3.264-3.214 (*m*, 2H, CH_2), δ 2.717-2.683 (*m*, 2H, CH_2), δ 2.042 (*s*, 2H, CH_2), δ 1.511-1.264 (*m*, 20H, 10(CH_2)), δ 1.042 (*s*, 9H, 3(CH_3)), δ 0.905-0.871 (*t*, 3H, CH_3). ^{13}C = δ (ppm) 171, 50, 42, 39, 33, 31, 30, 29.8-29.2, 26, 22, 14.

FT-IR, cm^{-1} (KBr) – 3301, 2955, 2919, 2851, 1634, 1544, 1469, 1365, 1344, 1265, 1233, 1149, 817, 718, 663, 619.

^{1}H, ^{13}C NMR

TBA1

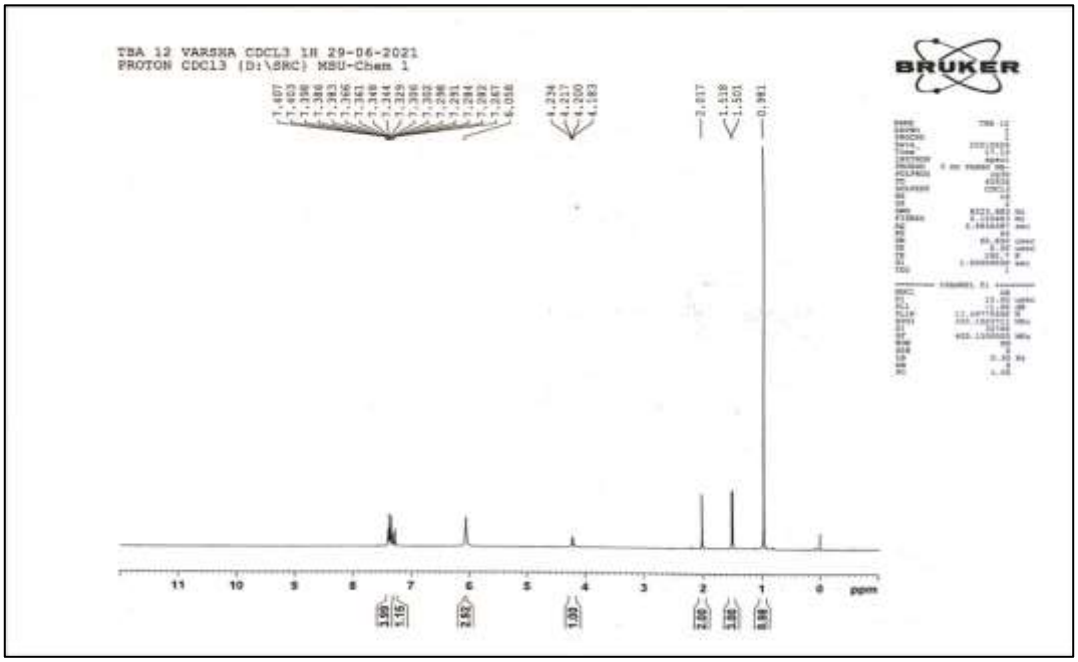

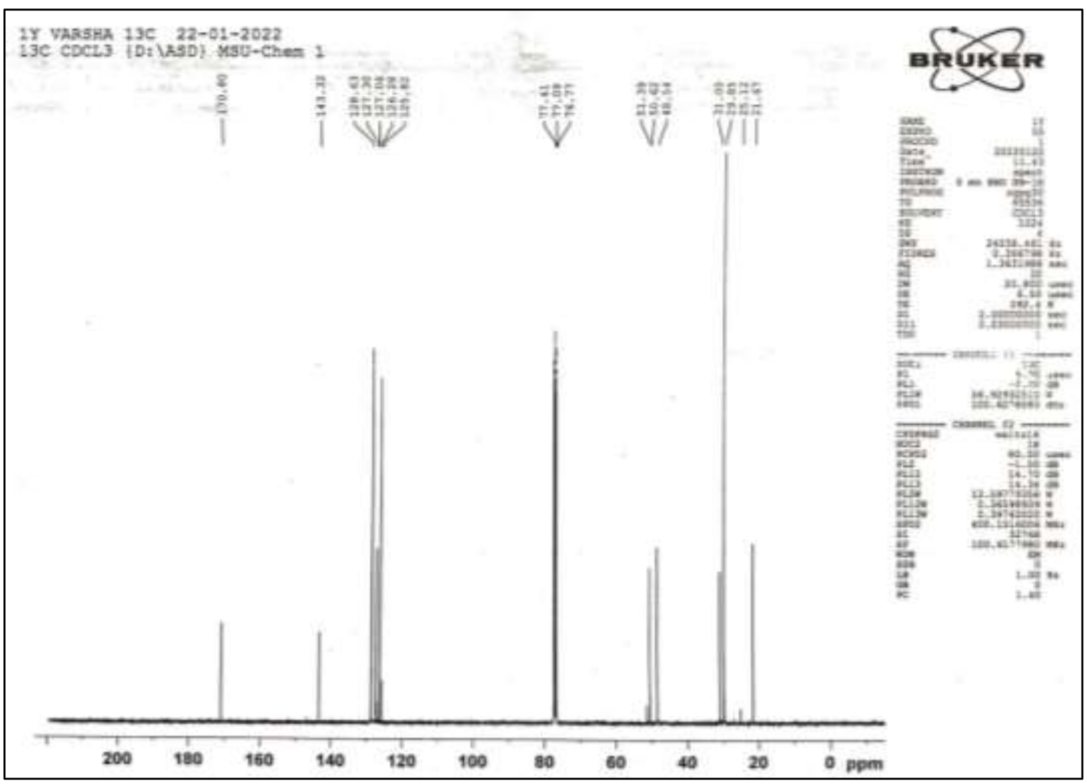

TBA2

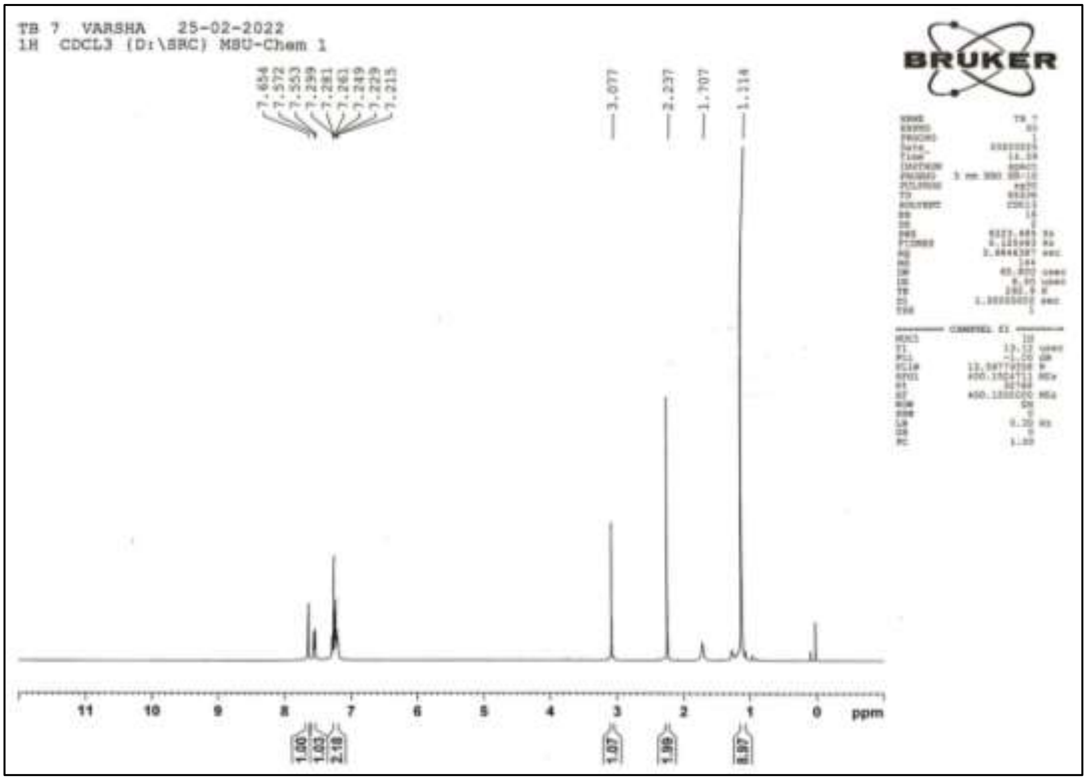
TB 7 VARSHA 25-02-2022
1H CDCL3 (D:\SRC) MSU-Chem 1
7.654
7.572
7.553
7.299
7.281
7.261
7.249
7.229
7.215
3.077
2.237
1.707
1.114
BRUKER
11
10
9
8
7
6
5
4
3
2
1
0
ppm
1.00
1.03
2.18
1.07
1.99
8.97

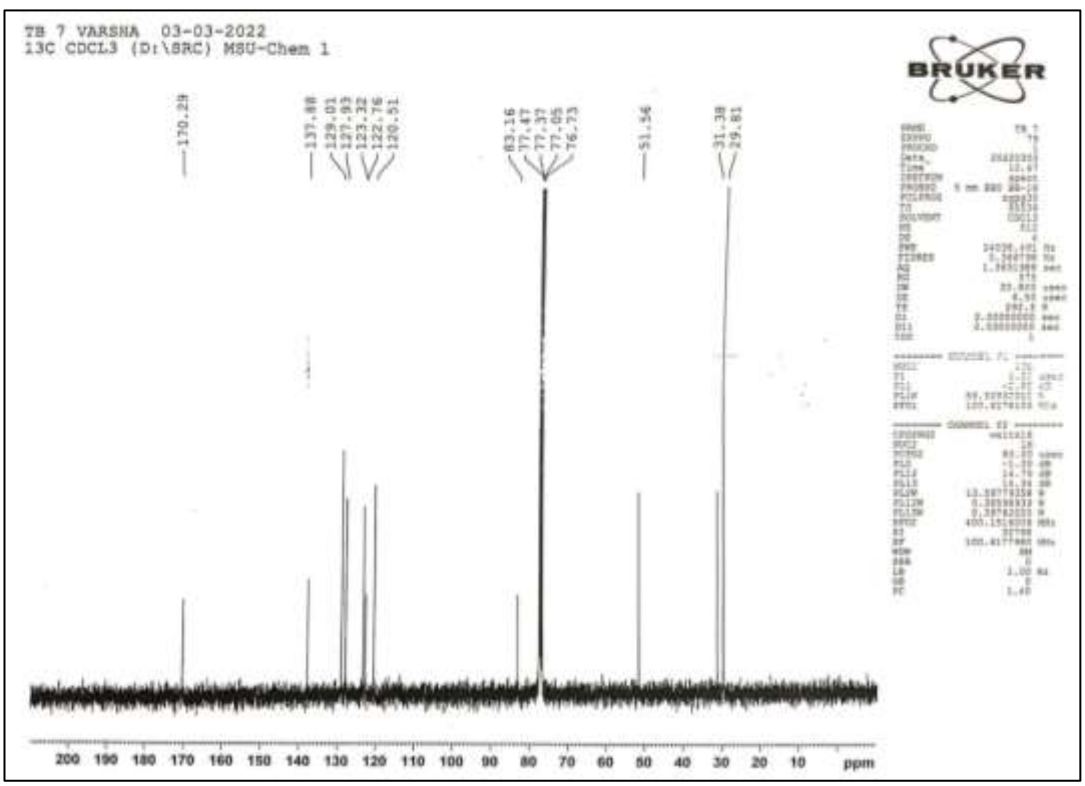
TB 7 VARSHA 03-03-2022
13C CDCL3 (D:\SRC) MSU-Chem 1
170.29
137.88
129.01
127.93
123.32
122.76
120.51
83.16
77.47
77.37
77.05
76.73
51.54
31.38
29.81
BRUKER
200
190
180
170
160
150
140
130
120
110
100
90
80
70
60
50
40
30
20
10
ppm

TBA3

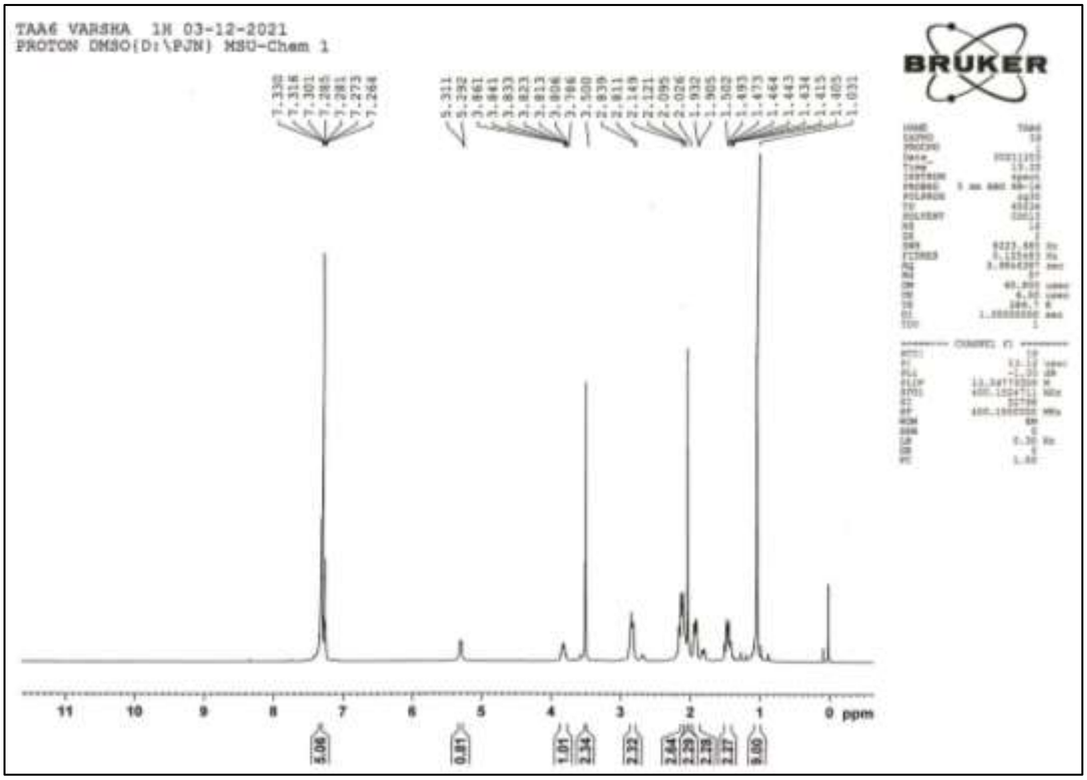
TAA6 VARSHA 1H 03-12-2021
PROTON DMSO(D:\PJN) MSU-Chem 1
BRUKER
7.330
7.316
7.301
7.285
7.281
7.273
7.264
5.311
5.292
3.861
3.841
3.833
3.823
3.813
3.806
3.786
3.500
2.839
2.811
2.149
2.121
2.095
2.026
1.932
1.905
1.502
1.493
1.473
1.464
1.443
1.434
1.415
1.405
1.031
11
10
9
8
7
6
5
4
3
2
1
0 ppm
5.06
0.81
1.01
2.34
2.32
2.64
2.29
2.26
2.17
9.00

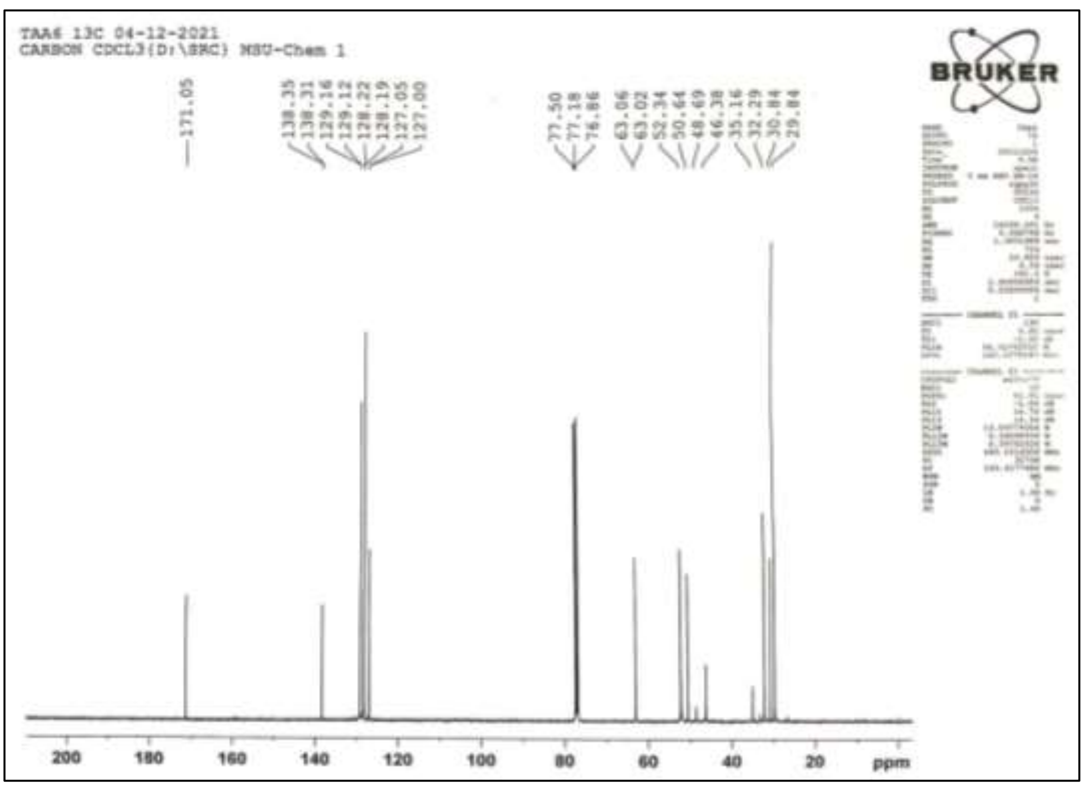
TAA6 13C 04-12-2021
CARBON CDCL3(D:\SRC) MSU-Chem 1
BRUKER
171.05
138.35
138.31
129.16
129.12
128.22
128.19
127.05
127.00
77.50
77.18
76.86
63.06
63.02
52.34
50.64
48.69
46.38
35.16
32.29
30.84
29.84
200
180
160
140
120
100
80
60
40
20
ppm

TBA4

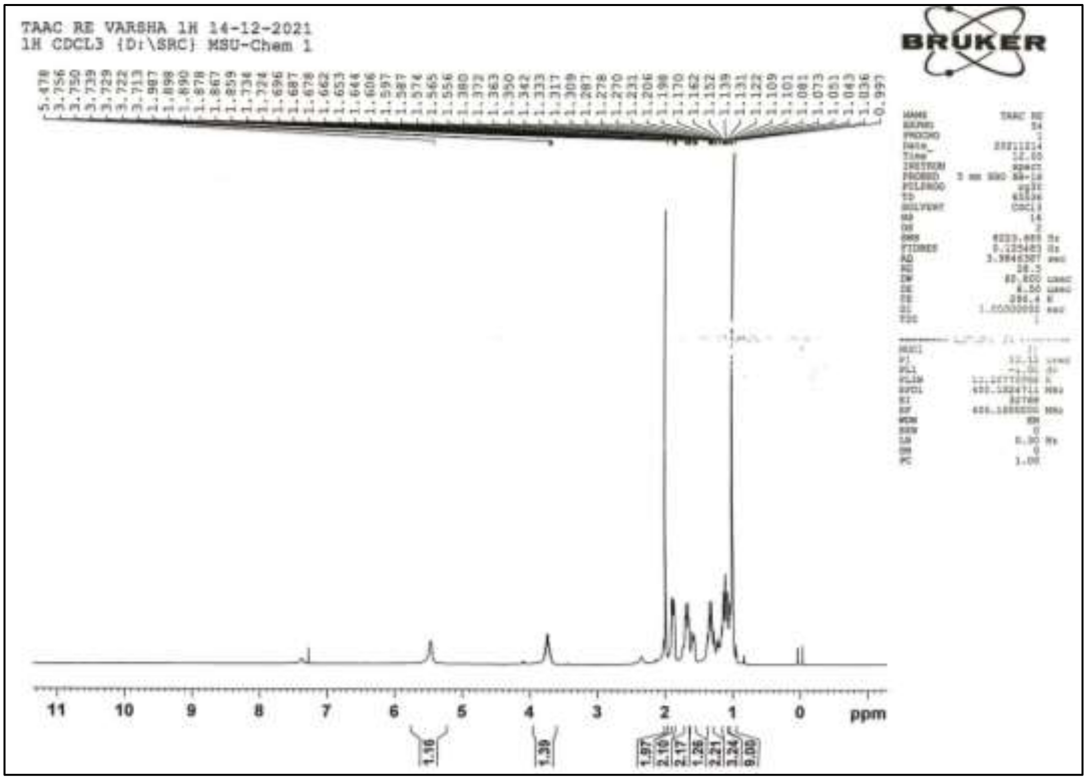
TAAC RE VARSHA 1H 14-12-2021
1H CDCL3 {D:\SRC} MSU-Chem 1
BRUKER
ppm

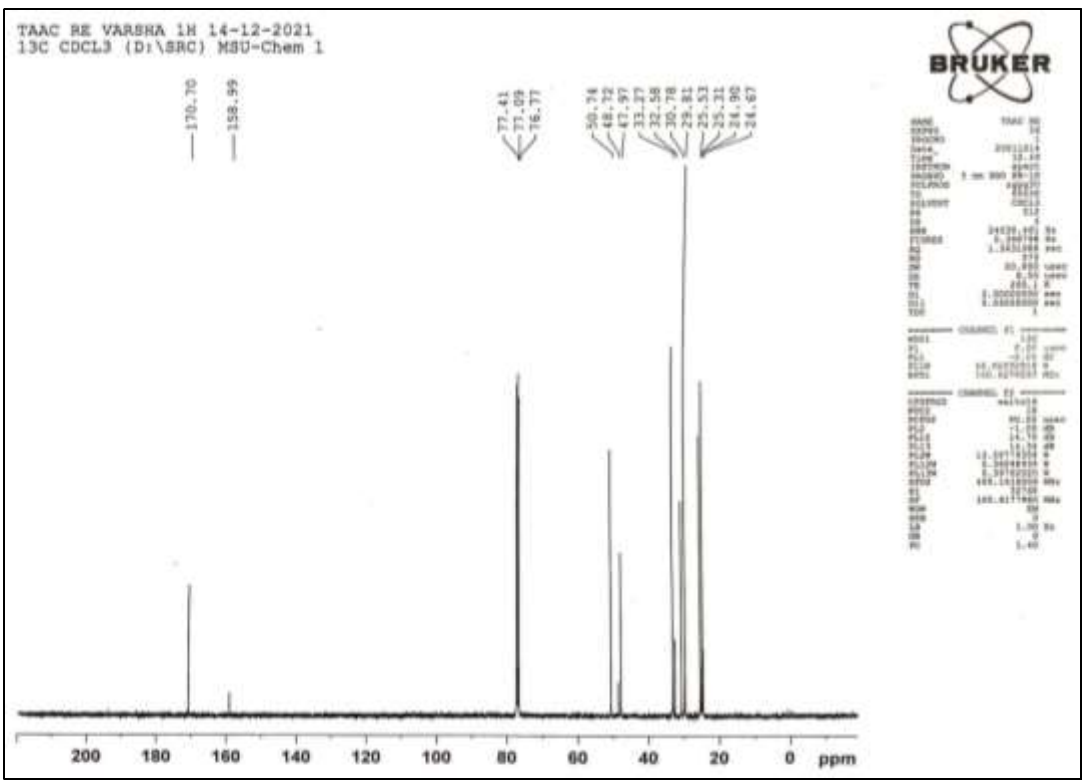
TAAC RE VARSHA 1H 14-12-2021
13C CDCL3 {D:\SRC} MSU-Chem 1
BRUKER
170.70
158.99
77.41
77.09
76.77
50.74
48.72
47.97
33.27
32.58
30.78
29.81
25.53
25.31
24.90
24.67
ppm

TBA5

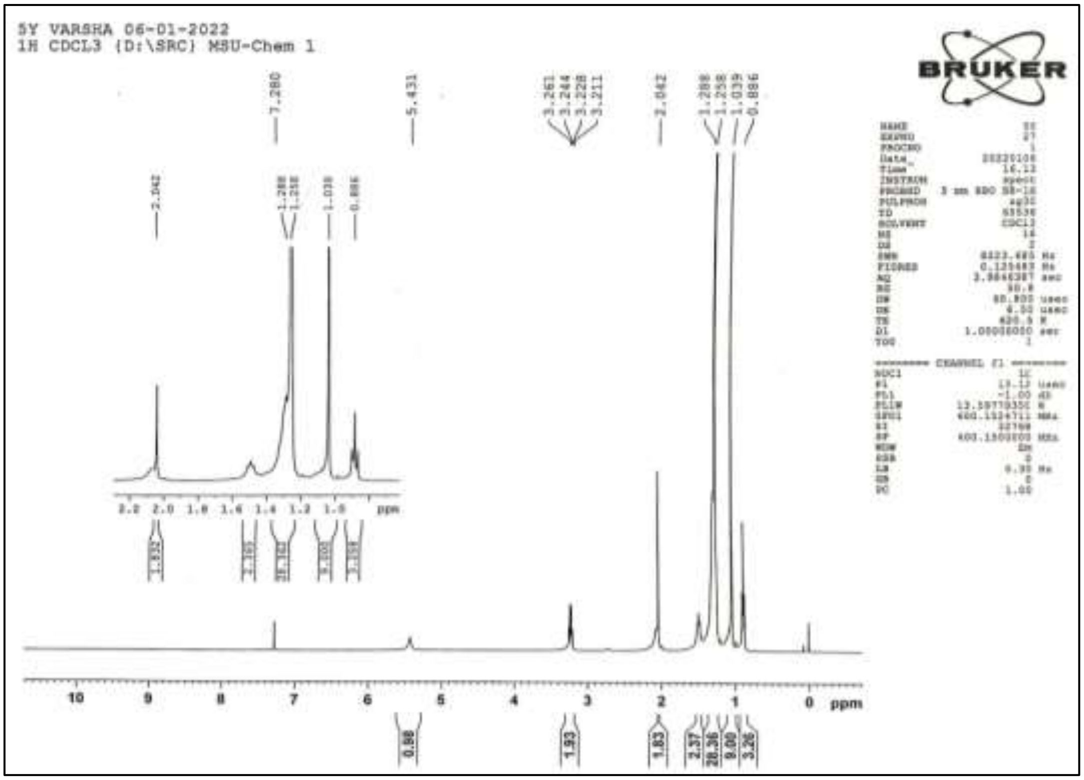

5Y VARSHA 06-01-2022
1H CDCL3 (D:\SRC) MSU-Chem 1
7.280
5.431
3.261
3.244
3.228
3.211
2.042
1.288
1.258
1.039
0.886
BRUKER
ppm
0.98
1.93
1.83
2.37
28.36
9.00
3.26

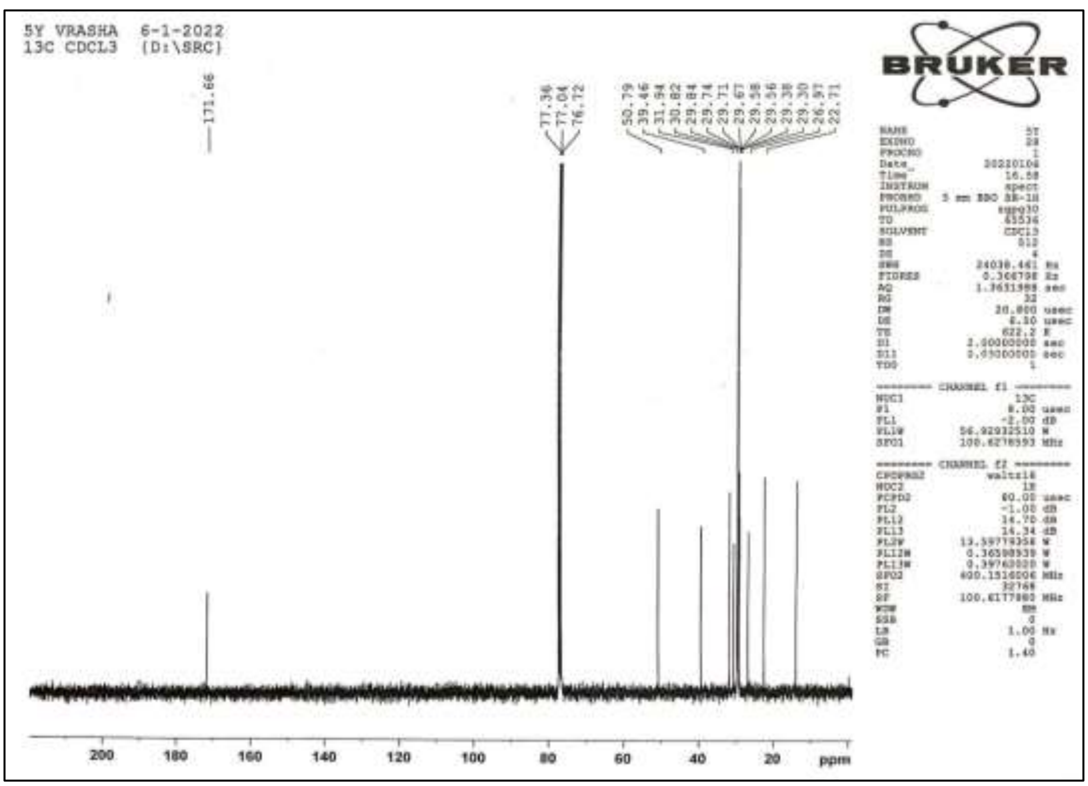

5Y VRASHA 6-1-2022
13C CDCL3 (D:\SRC)
171.66
77.36
77.04
76.72
50.79
39.46
31.94
30.82
29.84
29.74
29.71
29.67
29.58
29.56
29.38
29.30
26.97
22.71
BRUKER
ppm

TBA6

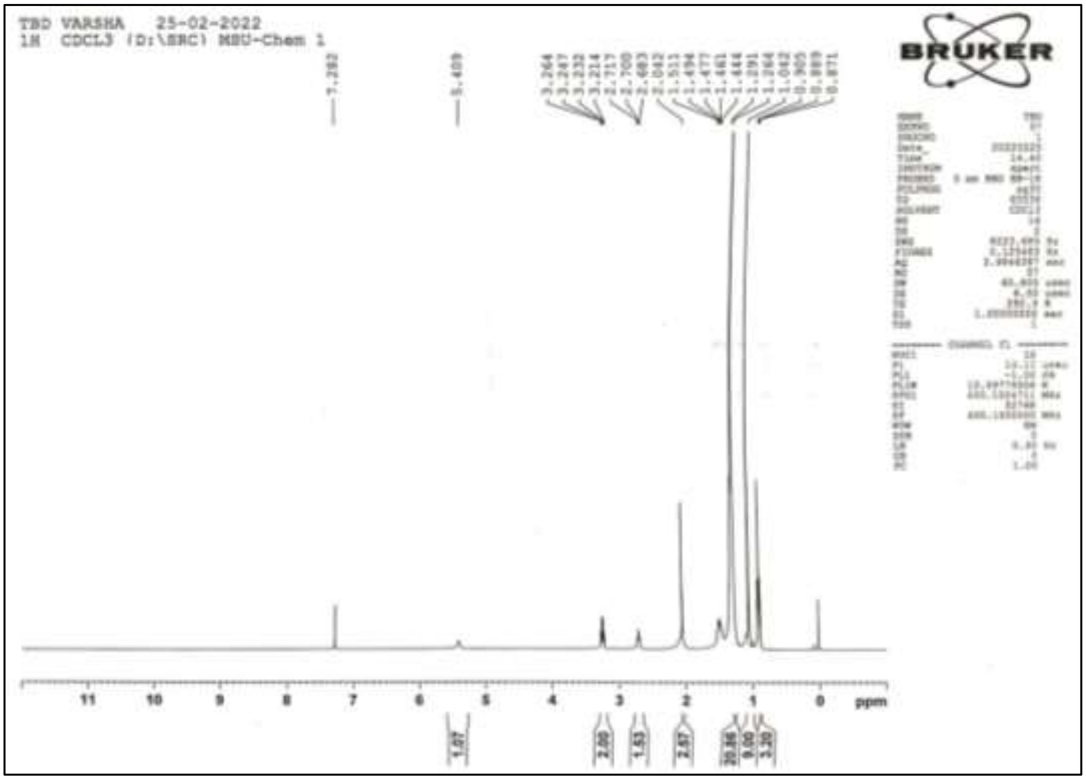
TBD VARSHA 25-02-2022
1H CDCL3 (D:\SRC) MSU-Chem 1
BRUKER
7.282
5.409
3.264 3.247 3.232 3.214 2.717 2.700 2.683 2.042 1.511 1.494 1.477 1.461 1.444 1.291 1.264 1.042 0.905 0.889 0.871
11 10 9 8 7 6 5 4 3 2 1 0 ppm
1.07 2.00 1.53 2.87 20.86 9.00 3.30

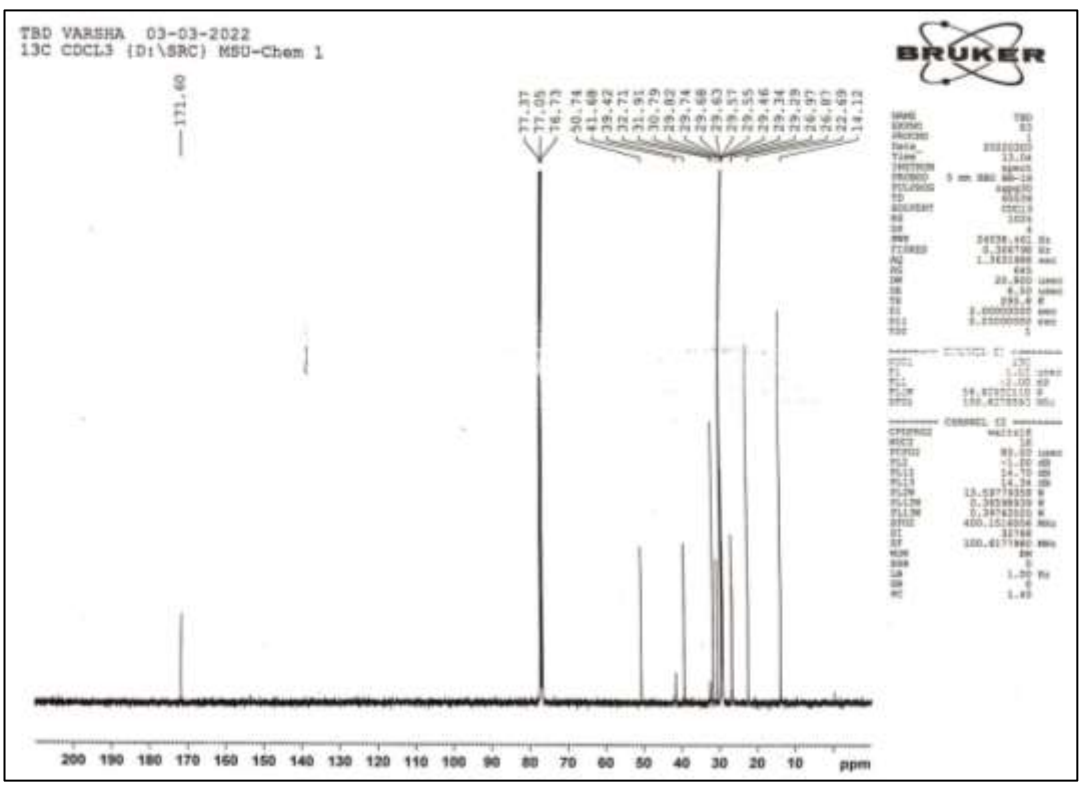
TBD VARSHA 03-03-2022
13C CDCL3 (D:\SRC) MSU-Chem 1
BRUKER
171.60
77.37 77.05 76.73
50.74 41.60 39.42 32.71 31.91 30.79 29.82 29.74 29.68 29.63 29.57 29.55 29.46 29.34 29.29 26.97 26.87 22.69 14.12
200 190 180 170 160 150 140 130 120 110 100 90 80 70 60 50 40 30 20 10 ppm

FT-IR

TBA1

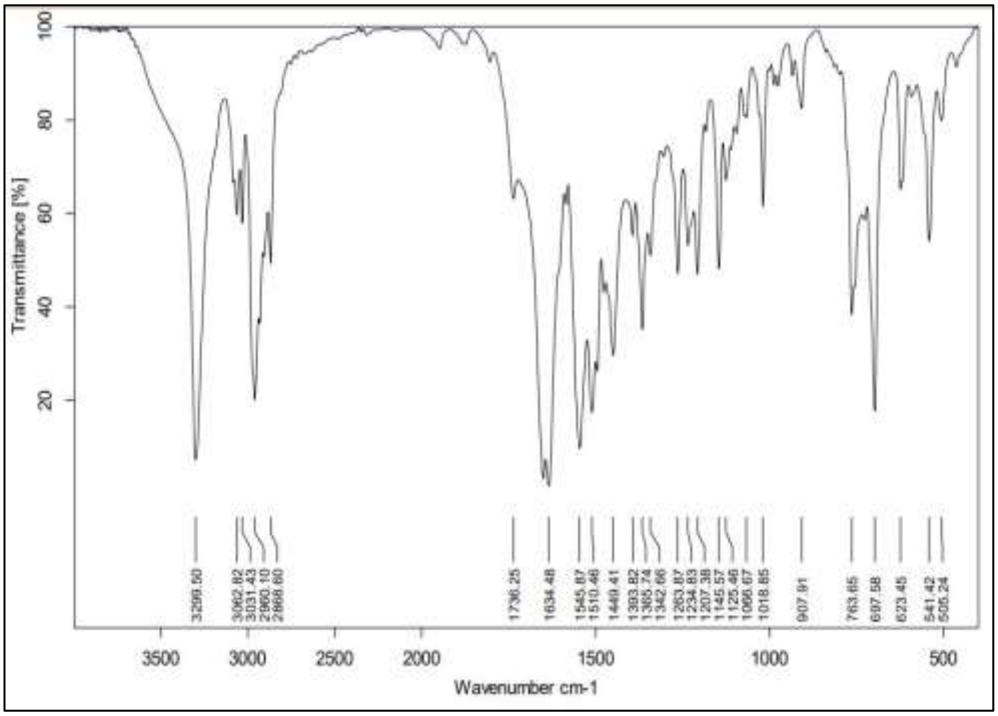

TBA2

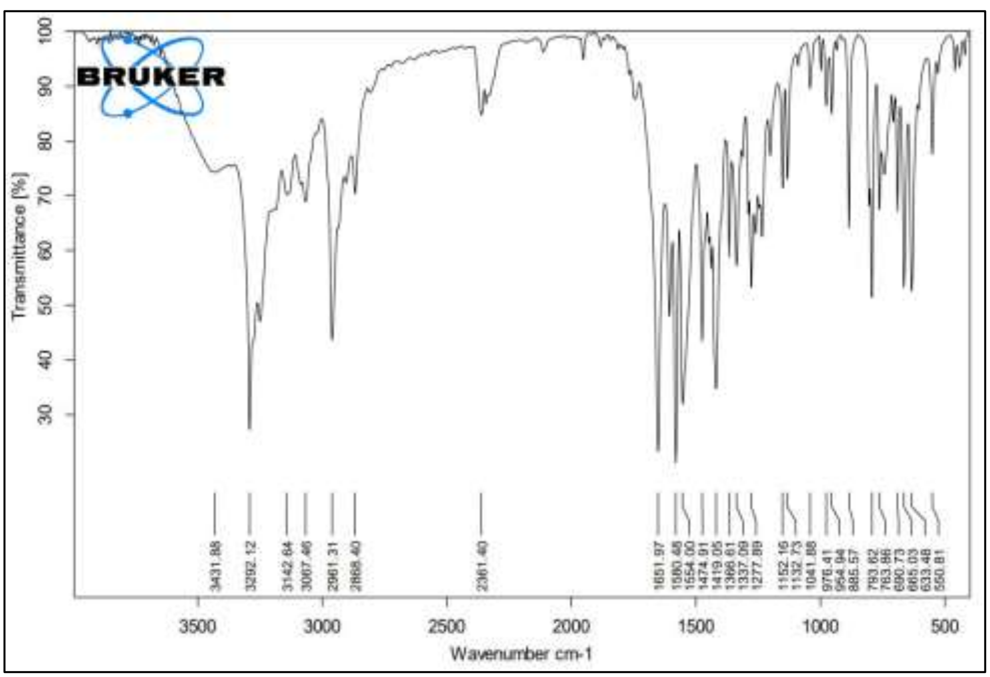

TBA3

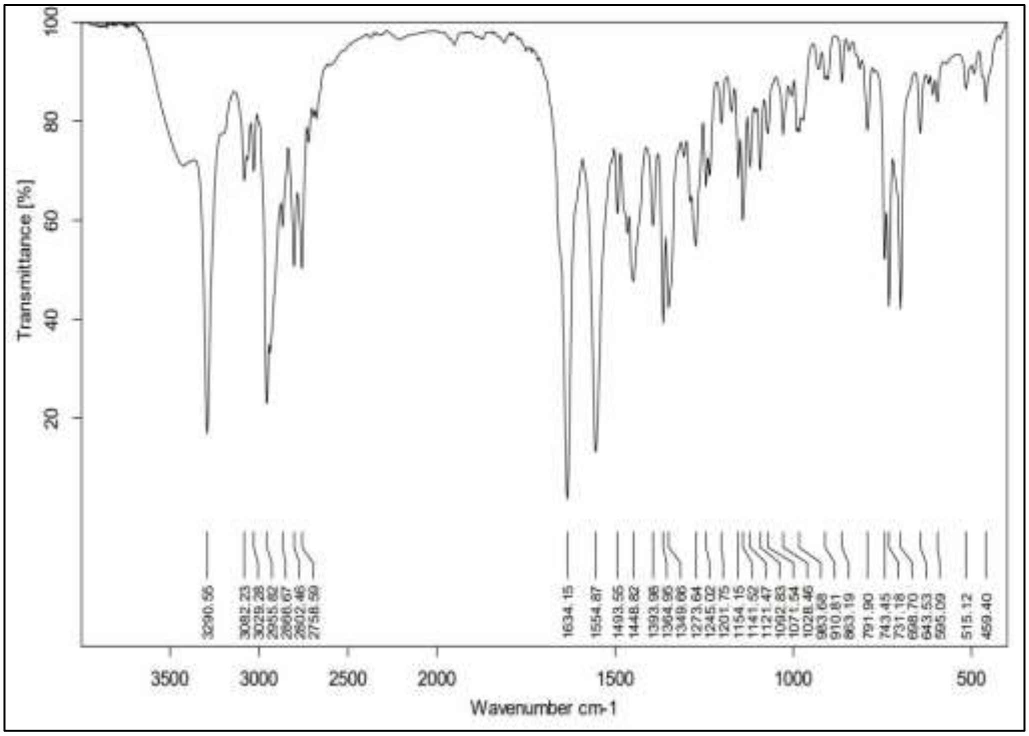
Transmittance [%]
100
80
60
40
20
3290.55
3082.23
3029.28
2955.82
2866.67
2802.46
2758.59
1634.15
1554.87
1493.55
1448.82
1393.98
1364.95
1349.66
1273.64
1245.02
1201.75
1154.15
1141.52
1121.47
1092.83
1071.54
1028.46
963.68
910.81
863.19
791.90
743.45
731.18
698.70
643.53
595.09
515.12
459.40
3500
3000
2500
2000
1500
1000
500
Wavenumber cm-1

TBA4

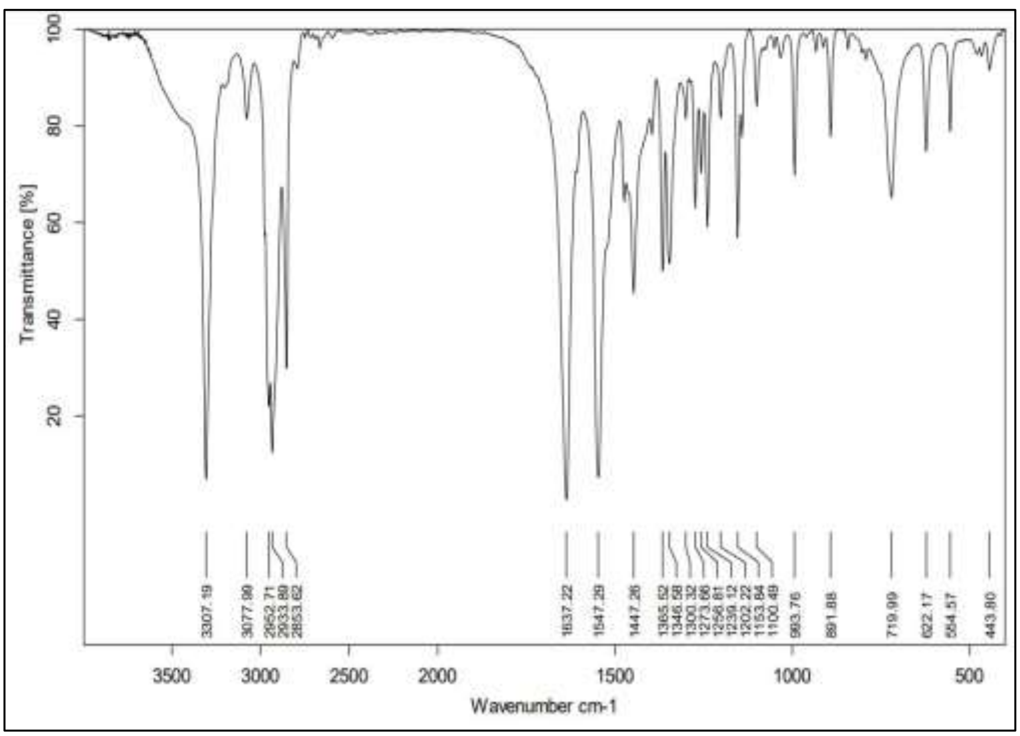
Transmittance [%]
100
80
60
40
20
3307.19
3077.99
2952.71
2933.89
2853.62
1637.22
1547.29
1447.26
1365.52
1346.58
1300.32
1273.66
1256.81
1239.12
1202.22
1153.84
1100.49
993.76
891.88
719.99
622.17
554.57
443.80
3500
3000
2500
2000
1500
1000
500
Wavenumber cm-1

TBA5

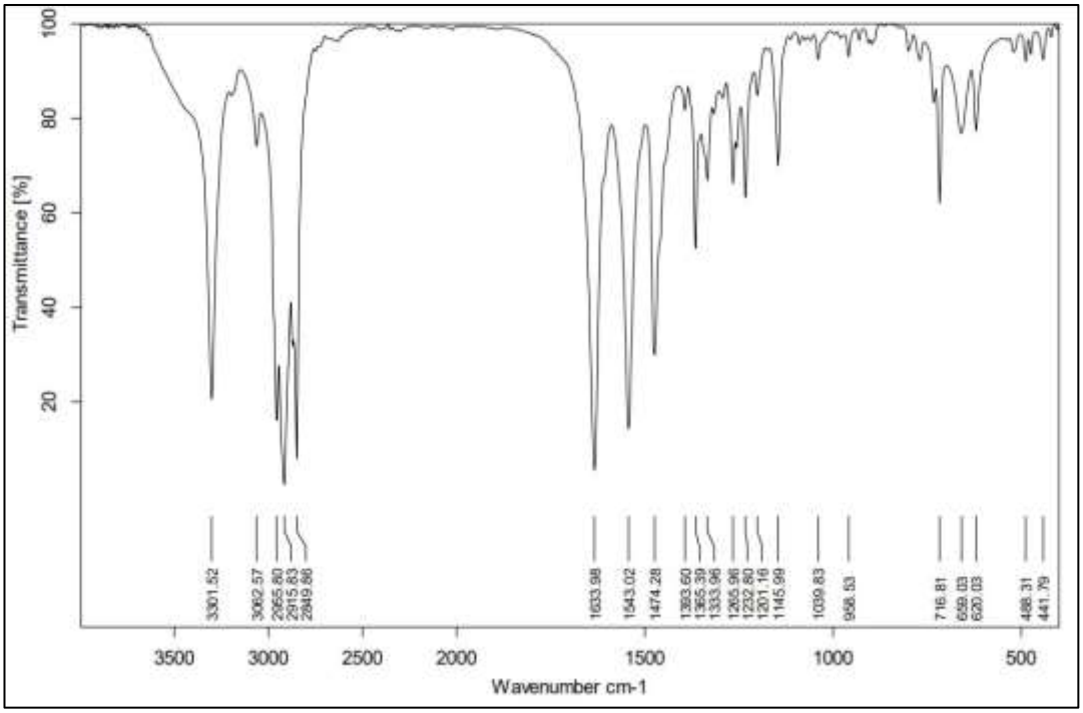
Transmittance [%]
100
80
60
40
20
3301.52
3062.57
2955.80
2915.83
2849.86
1633.98
1543.02
1474.28
1393.60
1365.39
1333.96
1265.96
1232.80
1201.16
1145.99
1039.83
958.53
716.81
659.03
620.03
488.31
441.79
3500
3000
2500
2000
1500
1000
500
Wavenumber cm-1

TBA6

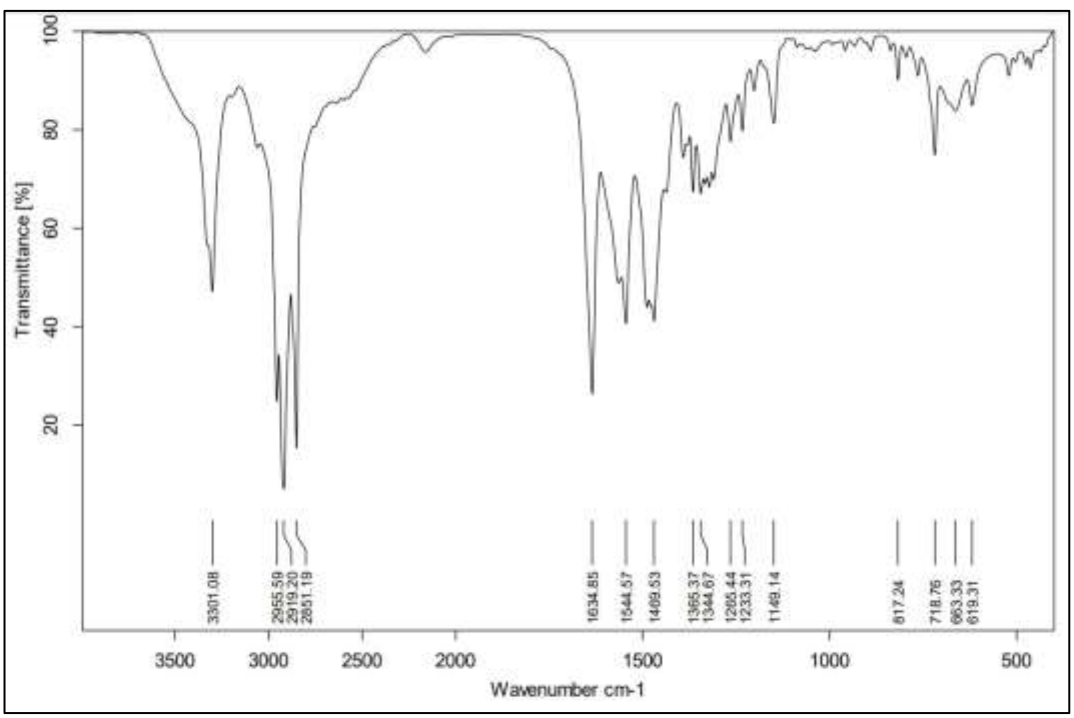
Transmittance [%]
100
80
60
40
20
3301.08
2955.59
2919.20
2851.19
1634.85
1544.57
1469.53
1365.37
1344.67
1265.44
1233.31
1149.14
817.24
718.76
663.33
619.31
3500
3000
2500
2000
1500
1000
500
Wavenumber cm-1